Doctorate Dissertation (Censored)

博士論文 (要約)

Development of Au-based Multinuclear Complexes with *N*-Heterocyclic Carbene Ligands

（*N*–ヘテロ環状カルベン（NHC）を支持配位子とする多核金錯体の開発）

A Dissertation Submitted for Degree of Doctor of Philosophy
July 2018

Department of Chemistry, Graduate School of Science,
The University of Tokyo

平成３０年７月博士（理学）申請
東京大学大学院理学系研究科 化学専攻

Qian Zhang
張　茜

Abstract

1. Introduction

Gold compounds have shown promise as catalysts for molecular transformation and luminescence materials. In particular, Au^I compounds have unique characteristics such as carbophilic π-acidity, redox activity, and aurophilicity due to the d^{10} closed shell electron configuration of Au^I ions in a linear two-coordinate geometry. Among them, multinuclear Au^I compounds, in which two or more Au^I ions are bonded or located close to each other, have been extensively investigated to gain knowledge about the influence of aurophilic interactions on the structure-specific electronic properties leading to multi-electron redox catalysts and photoluminescence. Over the last two decades, there has been a steep rise in research related to Au^I complexes ligated by *N*-heterocyclic carbene (NHC) ligands. Compared to traditional phosphine ligands, NHC ligands have a stronger σ-donating property, and manipulation of the electronic and steric characters of NHC ligands can be more easily achieved by *N*-functionalization. In this study, I focused on the construction of multinuclear Au^I complexes with NHC ligands. Specifically, a carbon-centered CAu^I_6 cluster and a macrocyclic dinuclear Au^I compound based on bis-NHC ligands have been developed for Au-based multinuclear complexes with structure-specific properties.

2. Synthesis and characterization of carbon-centered Au^I complexes supported by NHC ligands

In my master course study, I constructed a carbon-centered Au^I cluster, $[C(Au^IL)_6]^{2+}$, supported by 1,3-diisopropylimidazol-2-ylidene (L = I*i*Pr) ligands by the reaction of $[(IiPrAu)_3O](BF_4)$ with (trimethylsilyl)diazomethane in CH_2Cl_2 in the presence of triethylamine to produce chemically stable dark-brown solid. Based on this, detailed characterization of the product and comparison with those of phosphine ligand supporting counterparts were conducted based on ^1H and ^{13}C NMR, ESI-MS, absorption/emission, and XRD analyses in this study.

A single crystal of $[C(AuIiPr)_6](BF_4)_2$ suitable for XRD measurement was obtained by slow evaporation from a CH_2Cl_2/*n*-hexane solution as a yellow block crystal. The Au^I cluster has an antiprism structure with D_{3h} symmetry, and the bond lengths of Au(1)–Au(1)' and Au(1)–Au(1)" are 3.0548(3) and 2.9282(3) Å, respectively. This result suggests strong Au-Au interactions in the cluster. The Au–Au distances are comparable to those of a triphenylphosphine supported counterparts (2.887(1)–3.226(1) Å). Notably, the whole crystal structure is not highly symmetrical due to the packing force arising from the bulky I*i*Pr ligands.

Photoluminescence measurement of $[C(AuIiPr)_6](BF_4)_2$ cluster in the solid state revealed that it is luminescent with green emission under irradiation of UV light (λ_{ex} = 370 nm). The emission had a longer wavelength (λ_{em} = 547 nm) compared with that of a triphenylphosphine supported carbon-centered cluster (λ_{em} = 537 nm). This difference may come from the stronger σ-coordination ability of NHC ligands (Figure 1). On the other hand, no emission was observed for

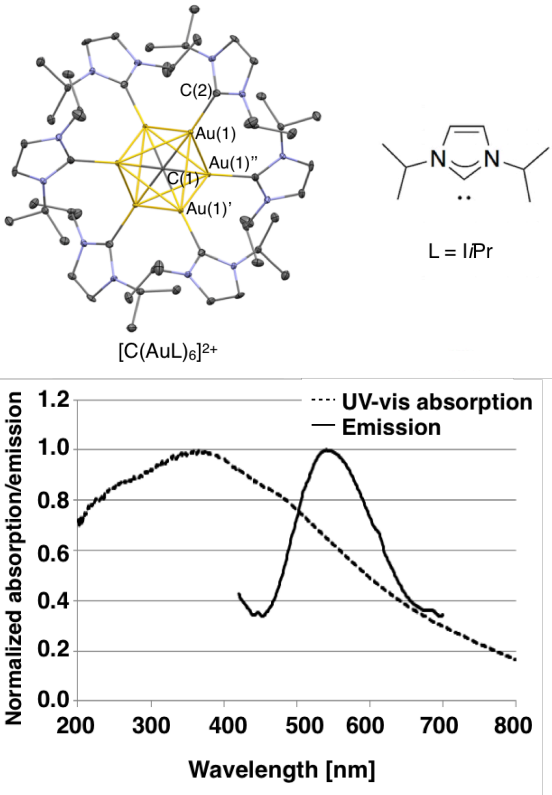

Figure 1. Upper: X-ray crystal structure of $[C(AuIiPr)_6]^{2+}$, bottom: UV-vis absorption (dash line) and emission spectra (bold line) of $[C(AuIiPr)_6](BF_4)_2$ in the solid state.

$[C(AuI\textit{i}Pr)_6](BF_4)_2$ in solution at room temperature.

3. Au-mediated macrocycle with bis-NHC ligands

NHCs can be easily modified with many types of organic ligand donors at the nitrogen atoms directing toward metal array. In this study, aiming at linearly arranging heterometallic coinage metal ions with a close distance to study the influence of metallophilic interactions on metal array-specific properties, I developed a bis-NHC ligand **L** with a pyridine-centered heterocycle-coupled spacer. Since NHC ligands have a higher affinity to Au^I ions than pyridine and furan, which prefer Ag^I or Cu^{II}, ligand **L** was expected to produce a linear heterometallic Au^I–M–Au^I (M = Ag^I or Cu^{II}) complex in a ladder or helical double-stranded structure.

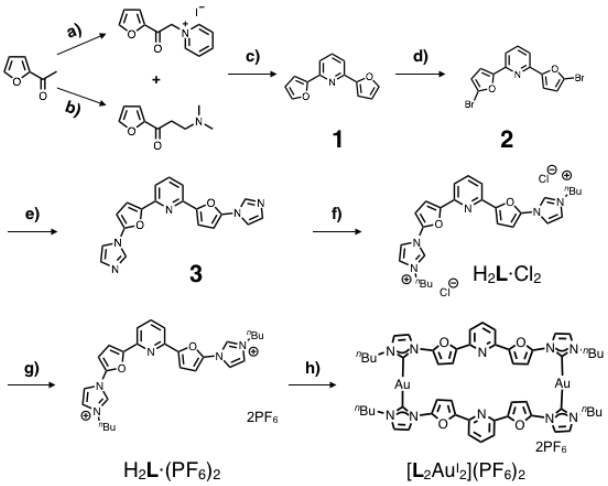

Scheme 1. a) I_2, Pyridine, reflux, 3 h, 98%; b) conc. HCl, $(CH_2O)_n$, $(CH_3)_2NH{\cdot}HCl$, EtOH, reflux, 16 h, then K_2CO_3, 90%; c) NH_4OAc, EtOH, reflux, 16 h, 21%; d) NBS, TsOH, benzene, 80 °C, 45 min, 67%; e) imidazole, *cat.* CuI, Cs_2CO_3, DMF, 120 °C, 60 h, 58%; f) *n*-BuCl, neat, 150 °C, 9 days; g) KPF_6, H_2O, rt, 98%; h) thtAuCl (1 eq), K_2CO_3, MeCN/DCM, rt, 8 h, 60%.

Ligand **L** was synthesized from 2-acetylfuran in 6 steps (Scheme 1). Firstly, 2,6-difuryl pyridine **1** was prepared by a coupling reaction of two 2-acetyl furan derivatives, and then brominated by *N*-bromosuccinimide (NBS) to afford **2**. Compound **2** was reacted with imidazole using a Cu^I catalyst to produce a bis-imidazole **3**, followed by alkylation at the terminal nitrogen atoms by *n*-butyl chloride to obtain a bis-imidazolium salt, $H_2\mathbf{L}{\cdot}Cl_2$. The counter anion was then replaced using $AgPF_6$ to obtain $H_2\mathbf{L}{\cdot}(PF_6)_2$. Complexation of $H_2\mathbf{L}{\cdot}(PF_6)_2$ with equimolar amount of thtAuCl (tht = SC_4H_8) in the presence of base formed a macrocyclic dinuclear Au^I complex, $[\mathbf{L}_2Au^I_2](PF_6)_2$ in 60% yield, which is air- and light-stable at room temperature. Its NMR spectra in $CDCl_3$ well established a high symmetrical structure in solution. The ^{13}C signals assignable to $C_{carbene}$ atoms were observed at 182.2 ppm, in the range for cationic two-coordinate NHC–Au–NHC compounds. The molecular structure of $[\mathbf{L}_2Au^I_2](PF_6)_2$ was determined by single-crystal X-ray analysis (Figure 2). The intramolecular Au–Au distance is *ca*. 13.5 Å, which is too far for intramolecular aurophilic interactions. Notably, as the macrocyclic cavity is very narrow and there is steric hindrance between the proton atoms on the furan rings, the Au^I-mediated macrocycle is distorted to adapt a helical structure while the single crystal is a racemic mixture.

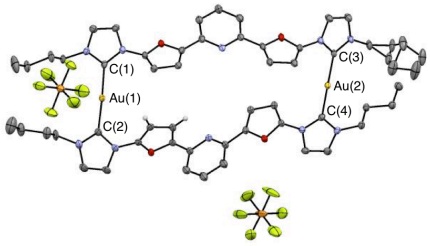

Figure 2. Single crystal X-ray structure ORTEP diagram of $[\mathbf{L}_2Au^I_2](PF_6)_2$ with 50% probability (H atoms are omitted for clarity). Selected bond lengths (Å) and angles (°): C(1)–Au(1) 2.020(6), C(2)–Au(1) 2.019(6), C(3)–Au(2) 2.015(6), C(4)–Au(2) 2.025(6), Au(1)–Au(2) 13.541, C(1)–Au(1)–C(2) 177.8(2), C(3)–Au(2)–C(4) 175.1(2).

$H_2\mathbf{L}{\cdot}(PF_6)_2$ and $[\mathbf{L}_2Au^I_2](PF_6)_2$ were investigated with respect to their photoluminescence properties (Figure 3). At room temperature, $H_2\mathbf{L}{\cdot}(PF_6)_2$ produced intense blue-purple luminescence both in solution and solid state. $[\mathbf{L}_2Au^I_2](PF_6)_2$ showed a photoluminescence behavior similarly to that of $H_2\mathbf{L}{\cdot}(PF_6)_2$, except that the intensity both in solution and solid state were much decreased. This result indicates that the emission mainly comes from the linked heteroaromatic rings, while significant quenching takes place in $[\mathbf{L}_2Au^I_2](PF_6)_2$ due to the steric and electronic changes caused by the complexation with Au^I ions.

The central pyridine moiety of the ligand **L** in $[\mathbf{L}_2Au^I_2](PF_6)_2$ can possibly coordinate to other metal ions to enable linear heterometallic arrangement. In expectation that a Cu^{II} ion would bridge two pyridine ligands in the macrocycle, 1.5 eq of Cu^{II} was added to a solution of $[\mathbf{L}_2Au^I_2](PF_6)_2$ in CH_3CN. However, instead of generation of $[\mathbf{L}_2Au^I_2Cu^{II}Cl_2](PF_6)_2$, oxidation of Au^I to Au^{III} was observed, as the signals for $\mathbf{L}_2Au^I_2$,

$\mathbf{L}_2Au^IAu^{III}$ and $\mathbf{L}_2Au^{III}{}_2$ were confirmed by NMR measurement (Figure 4). Further addition of Cu^{II} to the solution resulted in conversion from $[\mathbf{L}_2Au^I{}_2](PF_6)_2$ to a dinuclear Au^{III} macrocyclic compound $[\mathbf{L}_2Au^{III}{}_2Cl_4](PF_6)_2$. Unfortunately, the isolation of $[\mathbf{L}_2Au^{III}{}_2Cl_4](PF_6)_2$ was not successful because of its decomposition, as $\mathbf{L}_2Au^I{}_2$ and $\mathbf{L}_2Au^IAu^{III}$ species were observed again after purification probably due to their disproportionation. In order to fully study the redox behaviors of dinuclear macrocyclic compound $[\mathbf{L}_2Au^I{}_2]\cdot(PF_6)_2$ and to achieve redox-induced helicity switching in the solid state, later, freshly prepared dichloroiodobenzene as an oxidant was added to a solution of $[\mathbf{L}_2Au^I{}_2]\cdot(PF_6)_2$ in CH_3CN to generate fully oxidized dinuclear Au^{III} macrocyclic compound $[\mathbf{L}_2Au^{III}{}_2Cl_4]\cdot(PF_6)_2$, which was obtained as a stable white solid. Further study of the redox behavior and introduction of other heterometallic ions into macrocyclic $[\mathbf{L}_2Au^I{}_2](PF_6)_2$ is on going.

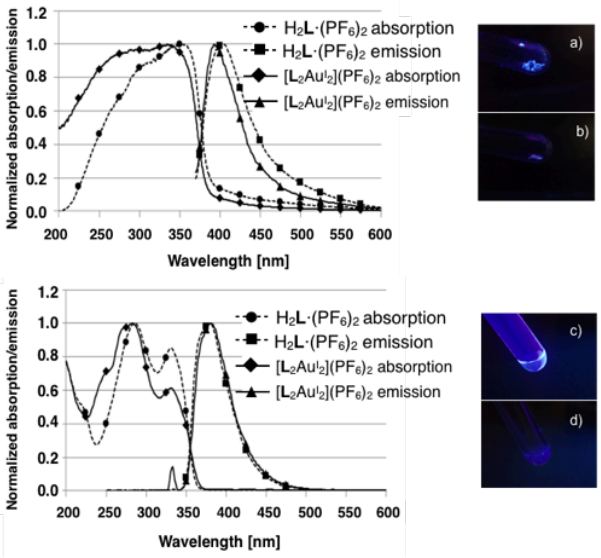

Figure 3. Upper: UV-vis absorption (dash line) and emission spectra (bold line) of $H_2\mathbf{L}\cdot(PF_6)_2$ and $[\mathbf{L}_2Au^I{}_2](PF_6)_2$ in the solid state upon excitation at 298 K. Bottom: UV-vis absorption (dash line) and emission spectra (bold line) of $H_2\mathbf{L}\cdot(PF_6)_2$ and $[\mathbf{L}_2Au^I{}_2](PF_6)_2$, in CH_3CN at a concentration of 10 μM, under aerobic condition at 298 K. Photographs: Luminescence of a) $H_2\mathbf{L}\cdot(PF_6)_2$ and b) $[\mathbf{L}_2Au^I{}_2](PF_6)_2$ in the solid state, c) $H_2\mathbf{L}\cdot(PF_6)_2$ and d) $[\mathbf{L}_2Au^I{}_2](PF_6)_2$ in CH_3CN at 5 mM, under aerobic condition at 298 K (365 nm).

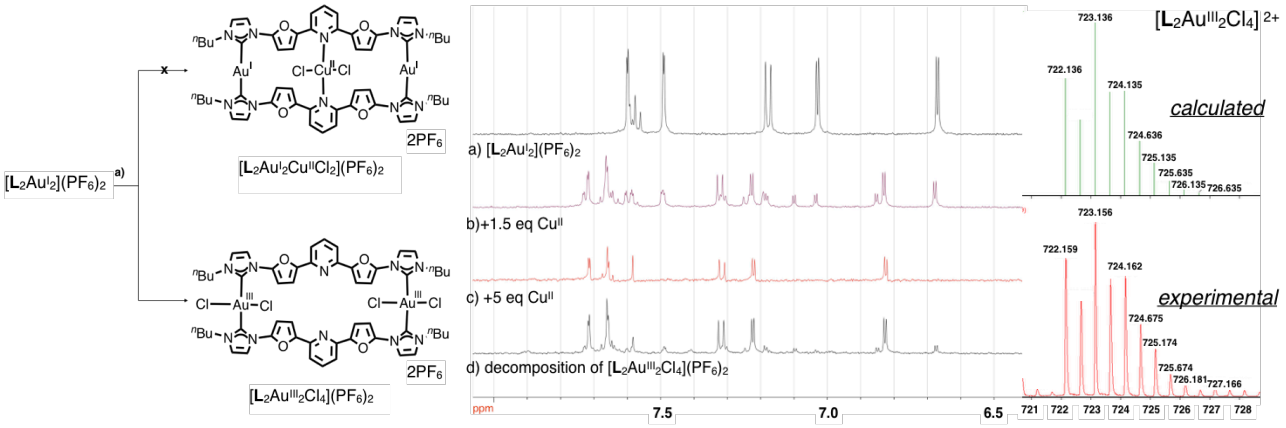

Figure 4. Left: Au^I centers oxidized by Cu^{II}, a) 5 eq of $CuCl_2$, CH_3CN, rt, 6 h; Middle: NMR spectrum of a) $[\mathbf{L}_2Au^I{}_2](PF_6)_2$, b) a mixture of $\mathbf{L}_2Au^I{}_2$, $\mathbf{L}_2Au^IAu^{III}$ and $\mathbf{L}_2Au^{III}{}_2$ species; c) $[\mathbf{L}_2Au^{III}{}_2Cl_4](PF_6)_2$ and d) decomposition of $[\mathbf{L}_2Au^{III}{}_2Cl_4](PF_6)_2$ during purification steps (500 MHz, 300 K, CD_3CN); Right: An ESI-TOF MS spectrum of $[\mathbf{L}_2Au^{III}{}_2Cl_4](PF_6)_2$ (positive, CH_3CN, 3000/30 V).

4. Conclusion

In this study, I have examined Au-based multinuclear complexes with *N*-heterocyclic carbene ligands using a carbon atom center or a linearly linking bis-monodentate ligand as the template, with a focus on the influence of carbene coordination and aurophilic interactions on the structure and electronic properties of the resultant complexes. Consequently, a carbon-centered CAu_6 cluster with antiprism arrangement as well as a macrocyclic dinuclear Au^I compound based on bis-NHC ligands were obtained and their luminescent properties and redox behaviors have been clarified. Further studies on their photochemical and electronic properties and multi-electron-based catalytic activities are now underway.

Abbreviations

conc.	concentrated
Cy	cyclohexyl
DFT	density functional theory
DMS	dimethyl sulfide
DMSO	dimethyl sulfoxide
eq	equivalent
ESI	electron-spay ionization
h	hours
Hz	hertz
J	coupling constant
L	ligand
i	*iso*
ICy	1,3-dicyclohexylimidazol-2-ylidene
I*i*Pr	1,3-diisopropylimidazol-2-ylidene
IMes	1,3-bis(2,4,6-trimethylphenyl)imidazol-2-ylidene
M	molar (mol/L)
min	minutes
MS	mass spectroscopy
m/z	mass-to-charge ratio
Me	methyl
n	normal
NHC	*N*-heterocyclic carbene
NMR	nuclear magnetic resonance
o	ortho
p	para
Ph	phenyl
Pr	propyl
ppm	parts per million
py	pyridyl
R	a functional group
rt	room temperature
t	tertiary
T	temperature
Tf	trifluoromethanesulfonyl

THF	tetrahydrofuran
TLC	thin layer chromatography
TMS	tetramethylsilyl
TOF	time-of-flight

Contents

1. General Introduction

1-1. Construction and application of Au^{I}-based multinuclear compounds

Gold has been an emblem of wealth and deeply involved in daily life throughout the ages. It is one of the most noble metals, and the price of gold is an important indicator of the worldwide financial status. Gold keeps its attractive and astonishing luster for incredible long period, without tarnishing on exposure to oxygen, moisture and light, and finds wide applications in many beautiful historical artifacts and works of art. On the other hand, due to its high elemental stability, the chemistry of gold has developed relatively slowly, in comparison with the other two coinage metals: silver and copper.[1]

Since early 1980s, gold chemistry has undergone extensive thriving; not only many well-developed areas of research have been improved, but also numerous creative approaches diversified the fields of research to an incredible extent. Nowadays, gold compounds have been flourishing in many fields, such as catalysts for molecular transformation and luminescent materials.[2] Among the most common and important oxidation states of gold, gold(I) chemistry with its extraordinary development and exploration represents a field full of challenges and opportunities. Gold(I) compounds have unique characteristics such as carbophilic π-acidity, redox activity and d^{10} closed-shell electron configuration of Au^{I} ions in a linear two-coordinate geometry.[3]

In the early 1980s, the general isolobality concept was firstly presented by Hoffmann, Stone, and Mingos, from then on, it has made a profound impact on the development of many fields of chemistry.[4] The frontier orbitals of LAu^{I} cation have similar symmetries and shapes as well as comparable energies with those of proton H^{+} and alkyl cations R^{+}. As a result, the isolobal analogy was mainly advanced for the LAu^{I} cation in gold chemistry. Not only the exploration of high-energy species in gas phase, but also the construction of a variety of Au-based clusters and aggregates with the main group as well as transition elements were inspired and guided by the isolobal principle. [5]

Since 1980's, construction of element-centered (boron, carbon, nitrogen, oxygen) multinuclear Au^{I} clusters supported by tertiary phosphine ligands has been extensively studied.[6] In these studies, hyper-auration of the element-centers occurred in most cases and the resultant cluster cations showed significant stability compared to their hyper-protonated or hyper-alkylated counterparts. These stabilization effects were

proposed to be a result of the intramolecular Au–Au contacts named as “aurophilicity”. In such clusters, the intramolecular Au–Au distances are typically in the range of 2.8–3.3 Å, well below the sum of the van der Waals radii (*ca.* 3.6 Å). The Au–Au contact is energetically comparable to that of standard hydrogen bonding, and therefore should serve as a key driving force for Au^{I}-based supramolecular architectures.[7]

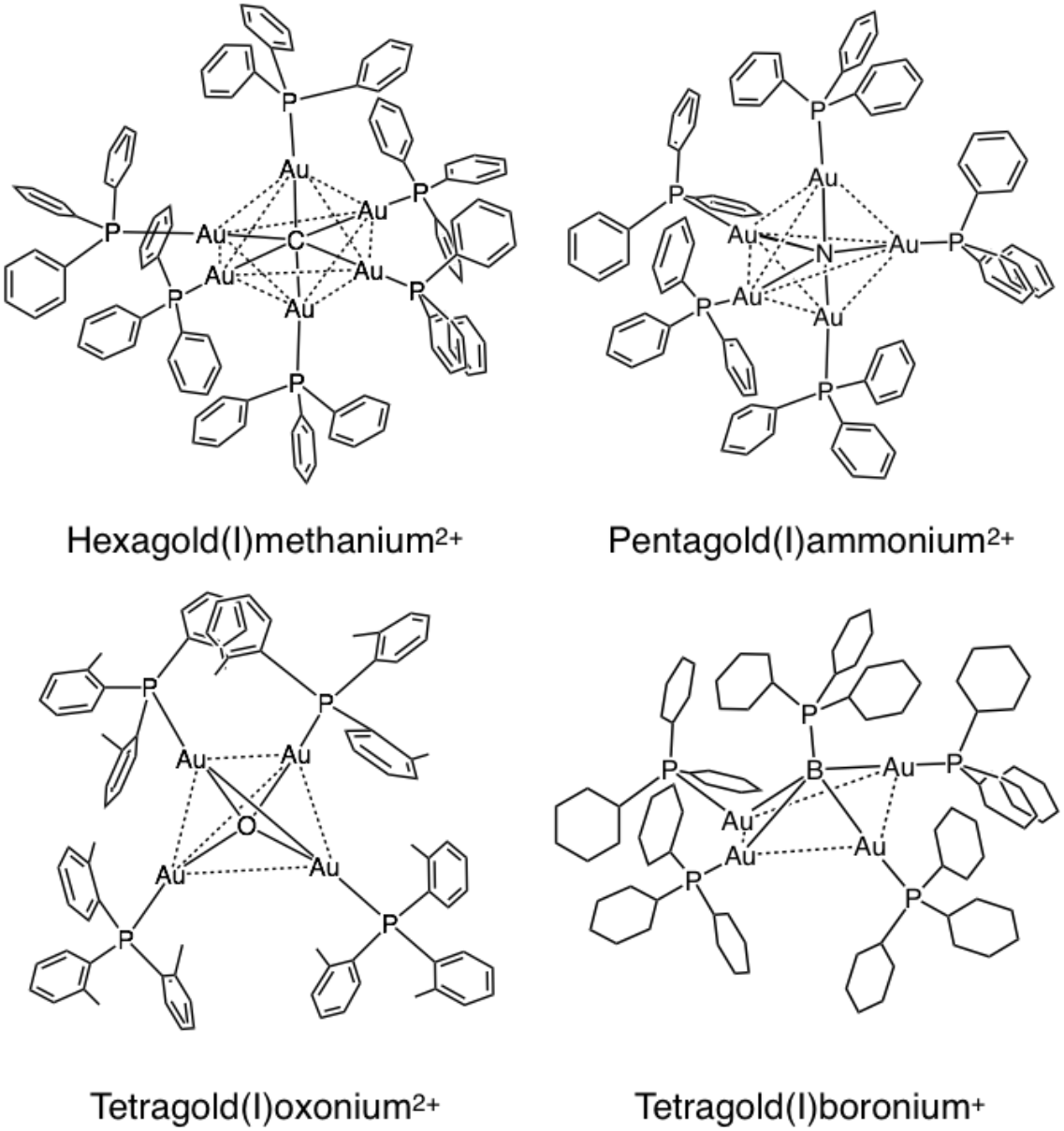

Figure 1-1-1. Element-centered Au^{I} clusters reported by Schmidbaur *et al*.

From then on, on the basis of the structure study, interests in the applications of multinuclear Au^{I} clusters also emerged at full speed, for instance, luminescent materials, catalysts for molecular transformation, and so on. Recently, multinuclear Au^{I} complexes

have become one of the most attractive candidates for various application studies, due to their stability and ready availability.[1,2]

Metal complexes exhibiting intense phosphorescence have attracted great attention for their possible applications as high-end materials.[9] Multinuclear Au^I complexes usually possess intense, long-lived luminescence with emission energies in the visible light range, thus studies in their luminescence properties are advantageous. Nowadays, the Au^I–Au^I interactions become more and more widely accepted as essential not only for constructing Au^I-based motifs with a wide range of structural diversity, but also for their electronic absorption and luminescence properties, in particular, in producing the emissive state.[9]

So far, as one of the fields that have been well studied, Au^I complexes have showed potential as a platform for the design of luminescent chemosensors due to their rich spectroscopic and luminescence properties. In 1998, Yam *et al.* reported a dinuclear Au^I complex with bridging diphosphines and benzocrown ether functionalized thiolate ligands. Addition of a potassium salt to the solution of Au^I complexes induced 'switching-on' of the intramolecular aurophilic interactions, thus gave rise to an intense red luminescence (Figure 1-1-2).[17]

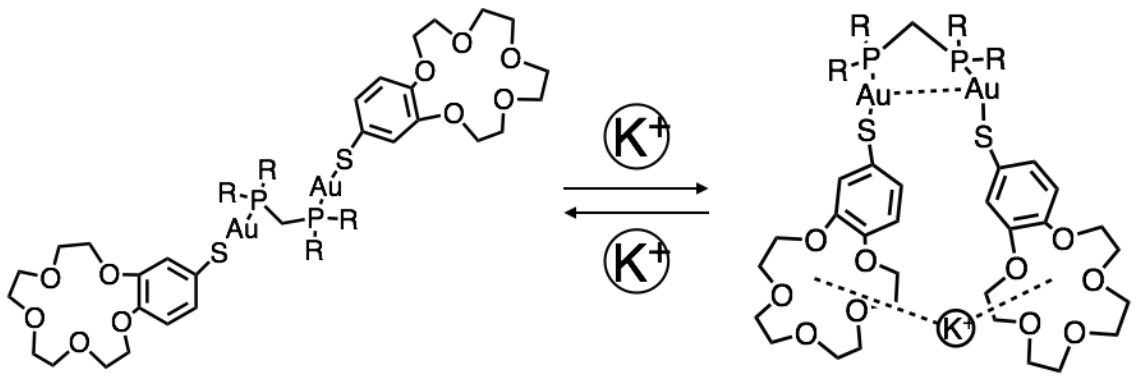

Figure 1-1-2. Potassium ions switch on and off of the intramolecular Au–Au interaction.

Moreover, the metallophilic interactions between Au^I and other closed-shell metal ions allow the extension of Au^I chemistry to mixed-metal compounds, increasing the structural diversity and variation of the final complexes. In many cases, the photoluminescence properties and potential applications were proven to be closely related to the presence of metallophilic interactions.

In 1997, Wang *et al.* reported a carbon-centered heterometallic $CAu^{I}_{6}Ag^{I}_{2}$ cluster using diphenylphosphpino-2-pyridine (dppy) ligands.[9] This heterometallic $CAu^{I}_{6}Ag^{I}_{2}$ cluster shows intense phosphorescence both in solution and in the solid state at room temperature, whereas the original homogenous CAu^{I}_{6} cluster supported by triphenylphosphine ligand shows weak emission in the solid state and no emission in solution. The authors assumed that increased rigidity by coordination of Ag^{I} ions and/or protection of $CAu^{I}_{6}Ag^{I}_{2}$ cluster by dppy ligand from quenchers in solution may cause the unusual luminescence of the $CAu^{I}_{6}Ag^{I}_{2}$ cluster (Figure 1-1-3).

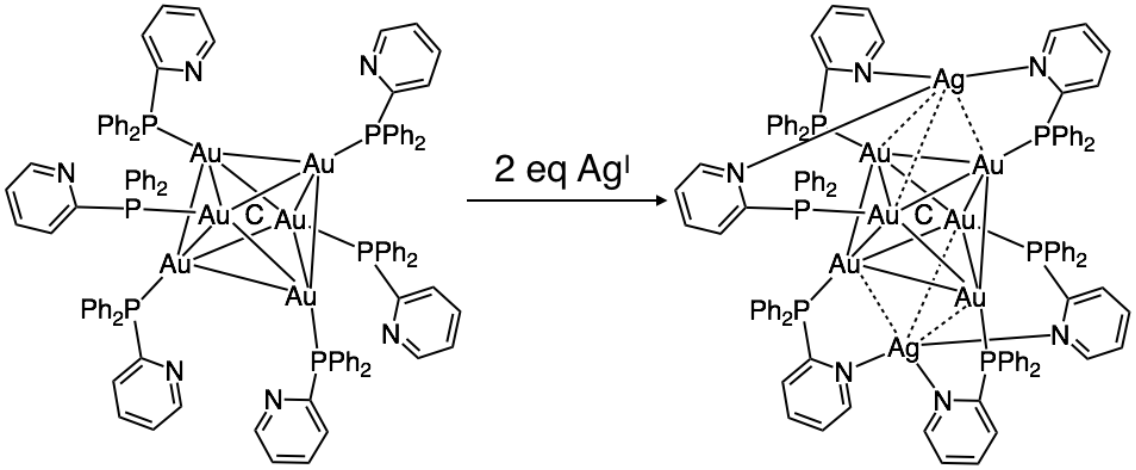

Figure 1-1-3. A carbon-centered heterometallic $CAu^{I}_{6}Ag^{I}_{2}$ cluster supported by diphenylphosphpino-2-pyridine (dppy) ligand reported by Wang *et al*.[9]

On the other hand, a great number of excellent papers have been reported on supramolecular structures based on Au^{I} complexes, most of them show inter- or intramolecular Au^{I}–Au^{I} interactions.[11] In a wide variety of Au^{I} frameworks, luminescence property is commonly observed. In 2014, Yam *et al.* reported a unique Au^{I}-containing supramolecular network, constructed from 3D cavitand-based coordination cages induced by Au^{I}–Au^{I} interactions (Figure 1-1-4). These Au^{I} supramolecular cages showed selective luminescence sensitivity toward Ag^{I} cation due to the strong Au^{I}–Ag^{I} metallophilic interactions.[12]

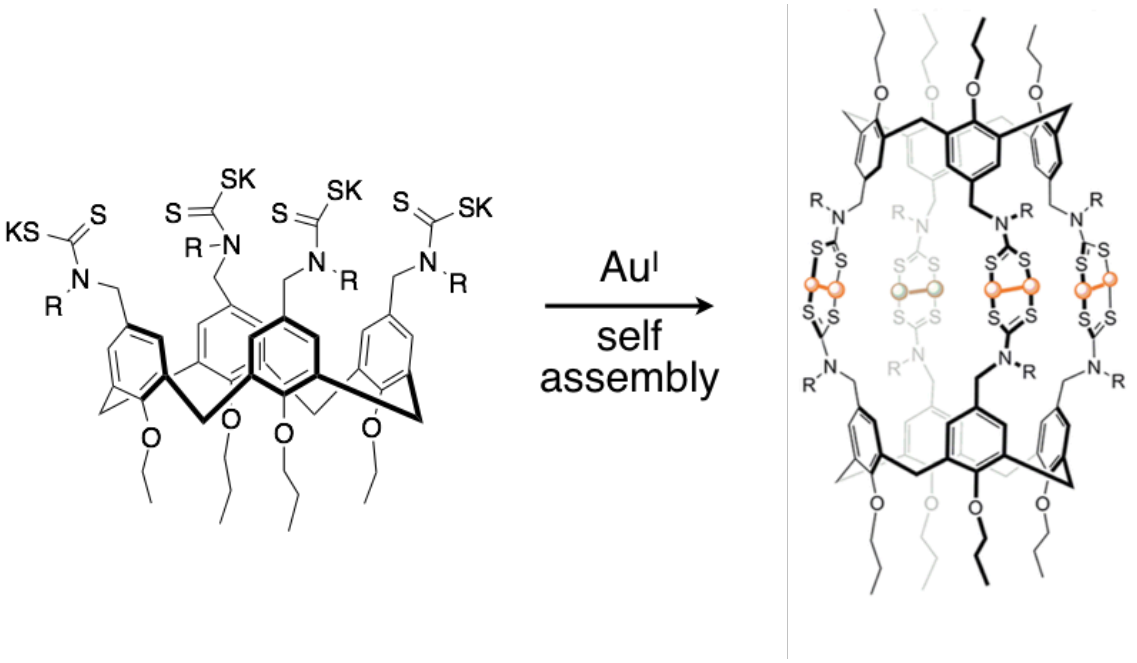

Figure 1-1-4. Construction of Au^{I}-containing metallo-supramolecular cages.

Homogeneous gold catalysis has become a "*hot topic*" due to its special catalytic character. So far, gold catalysis is mainly based on the Lewis acid properties of mononuclear Au^{I} and Au^{III} species. Recently, some multinuclear gold compounds have been reported as catalytically active species in homogeneous processes, which may be concerned with aurophilicity interactions and multi-electronic catalytic activities, so the mechanisms can be very different from those occurring under mononuclear Au center conditions. In 2016, Vlugt *et al.* have demonstrated that pre-organized two gold centers supported by a ditopic tridentate $PN^{H}P^{iPr}$ ligand is a suitable framework for dual σ, π-activation of functionalized alkynes by two gold centers.[14] In 2016, Echavarren *et al.* reported the synthesis of a tetranuclear Au^{I} complex and a heterometallic pentanuclear $Au^{I}_{4}Ag^{I}$ complex.[16] The homometallic Au^{I}_{4} complex undergoes C–H functionalization of carbonyl compounds, while the heterometallic $Au^{I}_{4}Ag^{I}$ is catalytically active for the carbonylation of primary amines to generate ureas (Figure 1-1-5). Also, Wang *et al.* reported that an $Au^{I}_{3}Ag^{I}$ oxo cluster bearing functionalized bis(2-pyridyl)phenylphosphine ligands can activate $C(sp^{3})$–H bonds of methyl ketones. Ag^{I} ions are very important for the catalytic activity, as attaching Ag^{I} ions results in more positive charges of the oxo cluster.[15]

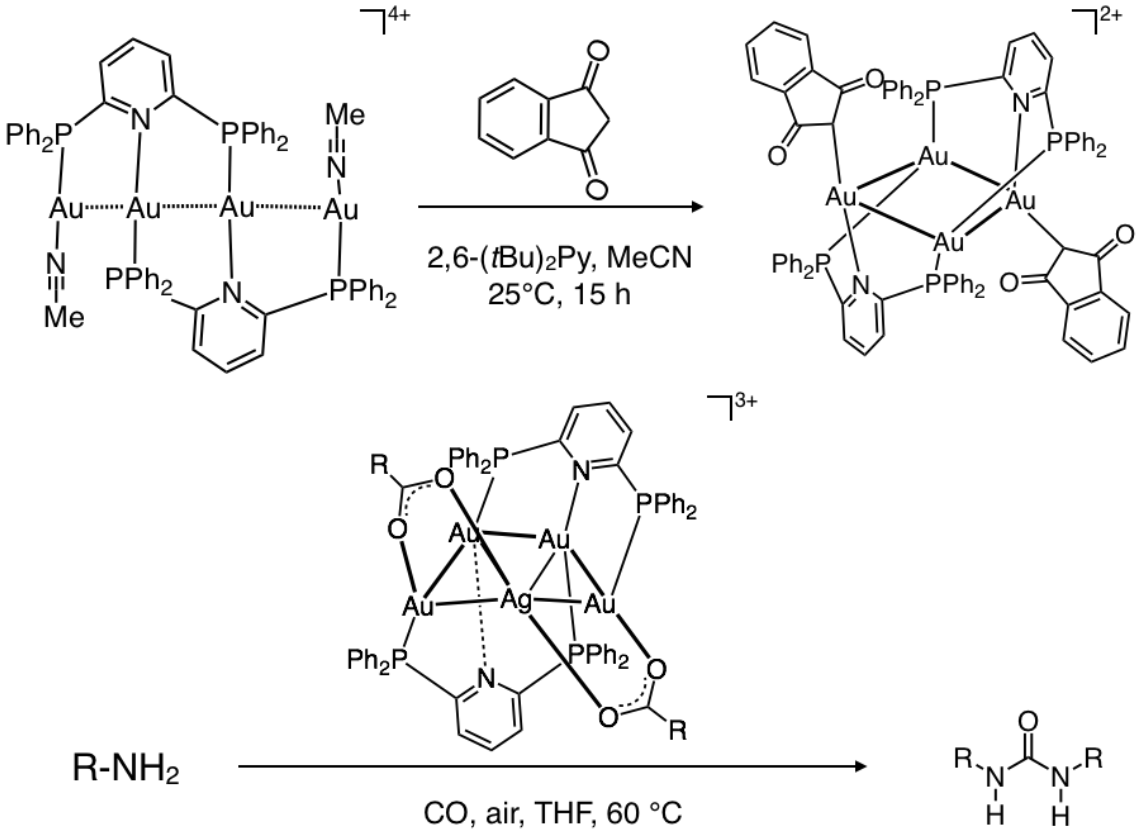

Figure 1-1-5. Catalytic activities of homo- and heterometallic Au^{I} clusters.

1-2. NHC-Au^I compounds

An *N*-heterocyclic carbene (NHC) contains a carbene carbon incorporated in a nitrogen-containing heterocycle. The first unequivocal isolation and subsequent crystal structure analysis of an *N*-heterocyclic carbene brought a lot of excitements to chemists.[19] In the last decade, the rise of *N*-heterocyclic carbenes has been so strongly-marked that almost all fields of organometallic chemistry have been influenced, and by now it has becoming a credible alternatives to the ubiquitous tertiary phosphines. It is widely believed that NHC ligands provide a metal center with high electron density due to σ-donation without any practical back-donation, since carbon is relatively soft and less electronegative than most heteroatom Lewis bases. Moreover, the p-orbital of carbene carbon participates in strong π-bonding with amino substituents. Unlike tertiary phosphine ligands, a structural alteration of substituents seems to cause a steric effect but only a minor perturbation of the electronic effect.[21]

Nowadays, gold complexes bearing an NHC ligand have attracted increased attention and shown potential applications in many fields. Previously, the procedures for the auration of imidazolium salts complexes have been exploited based on either free carbene or NHC transfer reagent like NHC-Ag^I complexes, but both reactions need harsh conditions. In 2013, Gimeno *et al.* reported a simple and efficient protocol for the preparation of ClAu(NHC) complexes, by direct treatment of imidazolium salts with weak bases such as K_2CO_3, in the presence of a gold transfer complex.[22] Owing to the easy synthetic procedure and ready stability, by now, NHC–Au^I complexes have become one of the most attractive candidates as pharmaceuticals, homogeneous catalysts, liquid crystals, and optical devices.

With NHCs a wide range of Au^I isolobal analogues have been prepared and well characterized, in which the phosphine-supporting congeners are still missing. The synthesis of gold hydride compound LAu-H was a real preparative challenge for many years.[23] In 2008, IPr (1,3-bis(2,6-diisopropylphenyl)imidazol-2-ylidene) was chosen as a supporting ligand for a Au^I hydride complex. In this work, stable complexes with a $(Au_2H)^+$ structure was also isolated and characterized (Figure 1-2-1).[24] These results have proved the stabilization imparted by NHC on the Au^I centers.

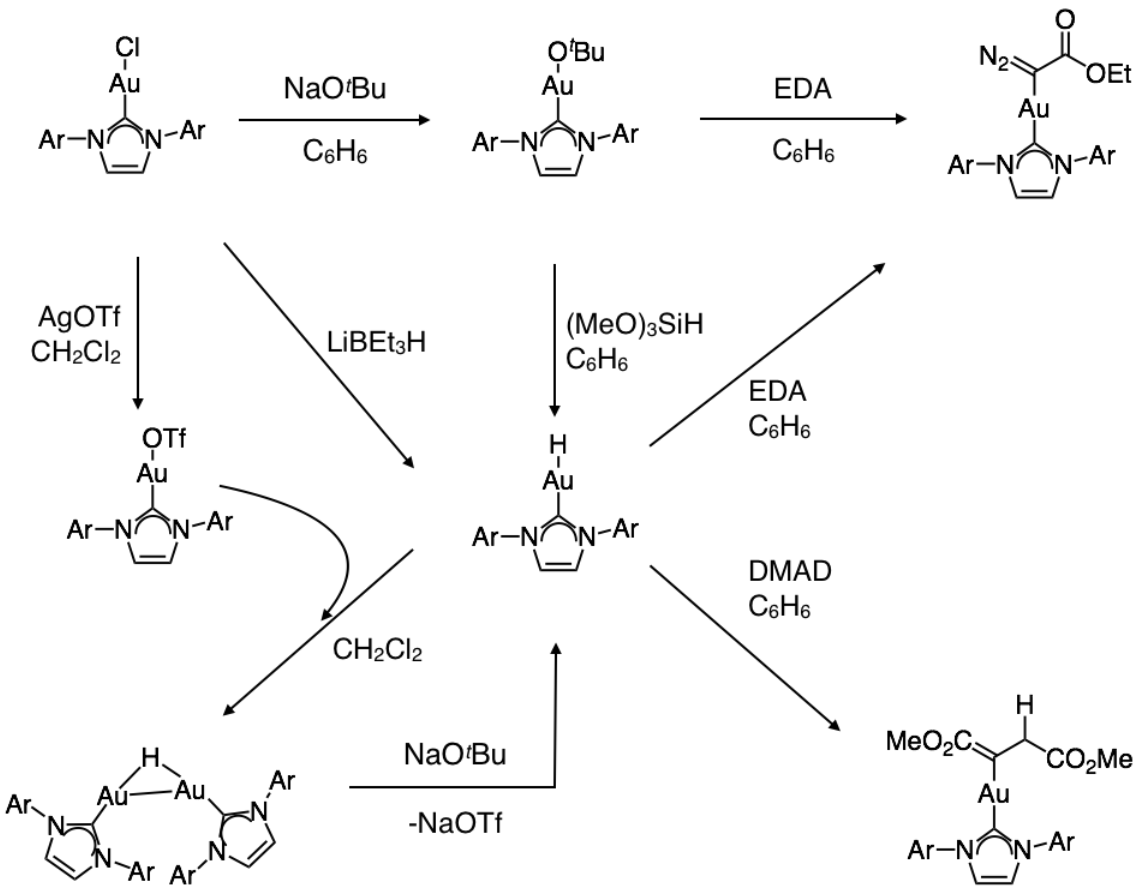

Figure 1-2-1. Synthesis and reactivities of a monomeric NHCAu^{I}-H complex.

More recently, Bertrand *et al.* reported the synthesis of a trinuclear mixed-valence Au^{I}/Au^{0} clusters supported by Cyclic(Alkyl)(Amino)Carbene (CAAC) ligands, through a simple ligand exchange reaction between the readily available μ^3-oxo-$[(Ph_3PAu)_3O]^+$ complex with free CAAC ligand (Figure 1-2-2). Free CAAC ligands, unlike free NHC carbene ligands, are stable and easy to handle under normal conditions. This mixed-valence Au cluster shows good availability to facilitate the catalytic carbonylation of amines.

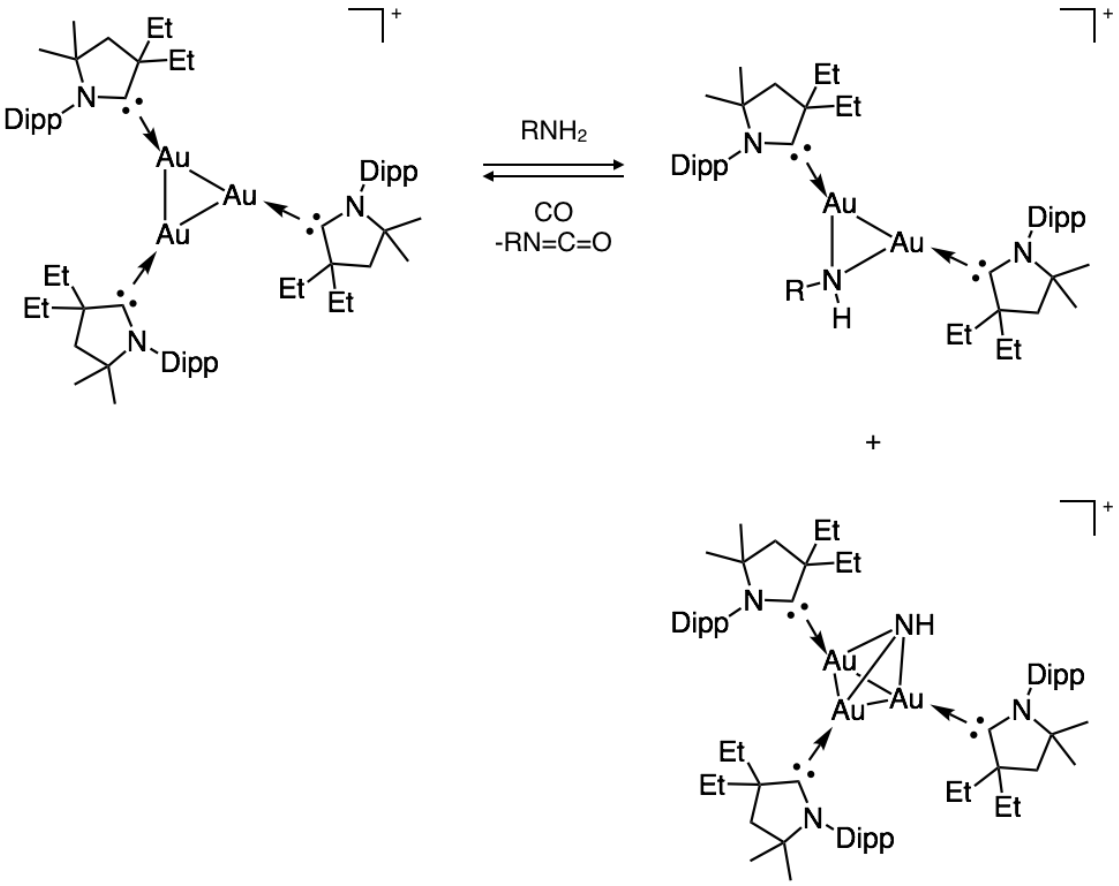

Figure 1-2-2. Addition of amines to a mixed-valence trinuclear $[Au_3]^+$ cluster and the subsequent reduction procedure.

Unlike other traditional ligands, for example, tertiary phosphines, NHCs are easily functionalized, as almost any organic substituent can be attached to the nitrogen atoms. Thus, donor sites such as phosphines, pyridines, alcohols, thiols, and other functional groups can be induced on purpose and allow a broad variety of applications for functionalized NHC complexes. NHC–Au^I complexes usually require the presence of either a chromophore group or extra donor sites that allow the formation of inter- or intramolecular metallophilic interactions to impart the desired luminescence. In 2010, Catalano *et al.* reported a bisNHC-Au^I complex that can manipulate its intramolecular metallophilic attractions for volatile organic compounds (VOC) sensing as shown in Figure 1-2-3.[27]

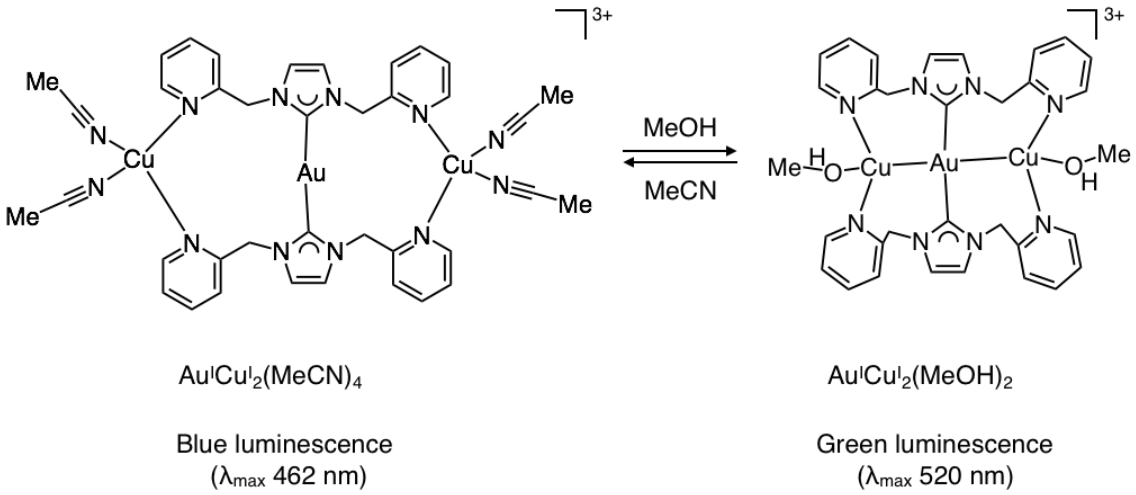

Figure 1-2-3. "On-Off" Au^{I}–Cu^{I} interactions in a bisNHC-Au^{I} luminescent vapochromic sensor.

In 2016, Braunstein *et al.* reported a series of homo- and heterometallic arrays constructed from a mononuclear Au^{I} cationic complex bearing a rigid bis(phosphine)-functionalized NHC ligand (Figure 1-2-4). The authors studied the effects of metallophilic interactions on photoluminescence behaviors experimentally in detail in this work.[28]

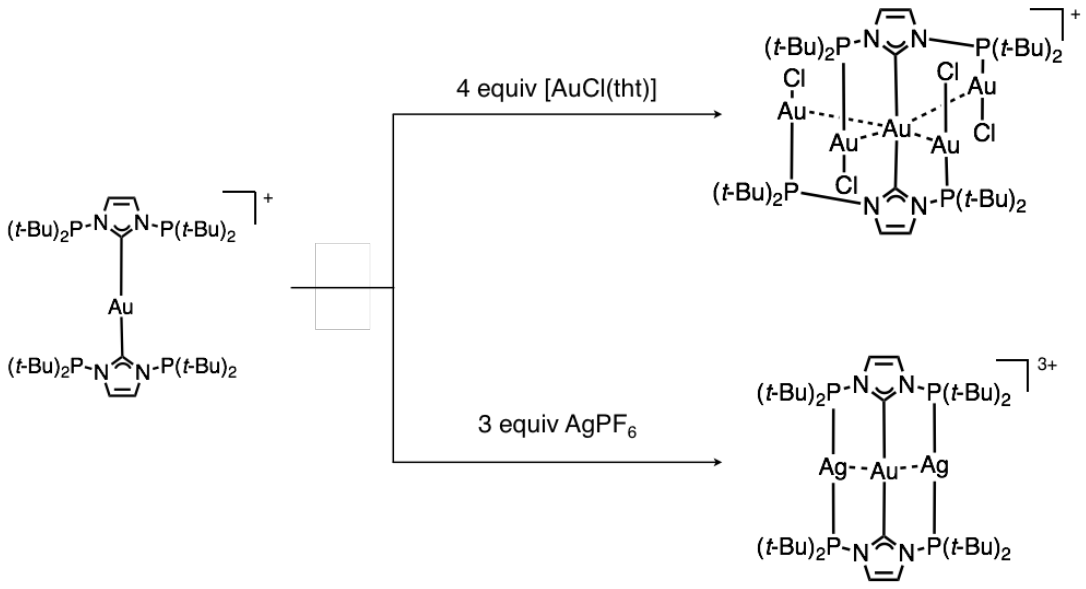

Figure 1-2-4. A bis(phosphine)-functionalized NHC ligand supported multinuclear Au^{I} and Au^{I}-Ag^{I} complexes.

Due to their excellent σ-donative ability, NHCs ligands have been widely used in homogeneous gold catalysis. Earlier Au^{I} systems bearing tertiary phosphine donor ligands generate the catalytic active Au^{I} species *in situ* through the traditional [Au(L)Cl]/silver salt methods. On the other hand, NHCs allow the isolation of reactive single-component intermediate systems. So far, activation of alkynes, allenes, and alkenes as well as carbonyl and aryl halide compounds has been extensively studied with NHC-based gold catalysts. In 2003, the very first example of catalytic use of an NHC-gold complex for the hydration of an alkyne was reported.[29] Later NHC ligands show it superiority in Au^{I} catalysis, as the use of the IPr ligand made it possible to run an intramolecular hydroamination reaction of the *N*-alkenyl acetamide at a lower temperature than those previously reported catalytic systems based on PR_3-Au^{I} complexes (Figure 1-2-6).

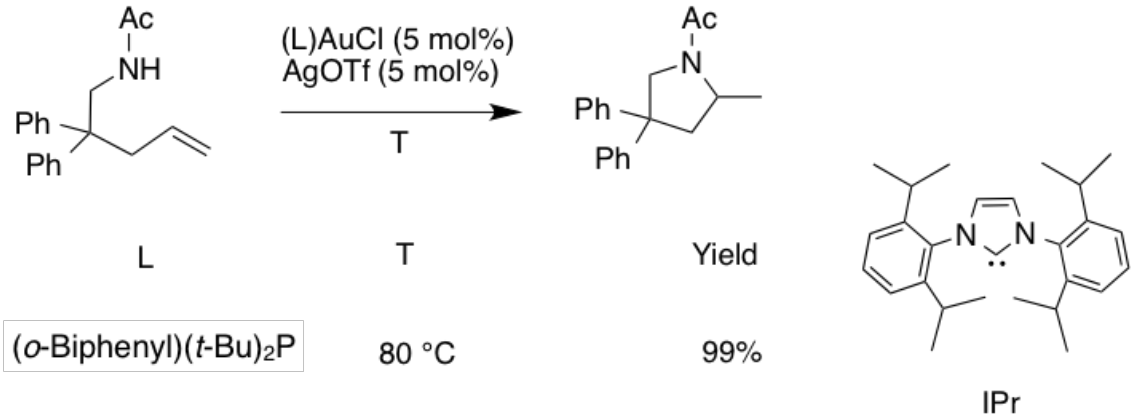

Figure 1-2-6. Gold-catalyzed intramolecular hydroamination.

1-3. The aim of this study

Gold compounds have shown promises as catalysts for molecular transformation and luminescent materials. In particular, Au^I compounds have unique characteristics such as carbophilic π-acidity, redox activity, and aurophilicity due to the d^{10} closed shell electron configuration of Au^I ions in a linear two-coordinate geometry. Among them, multinuclear Au^I compounds, in which two or more Au^I ions are bonded or located close to each other, have been extensively investigated to gain knowledge about the influence of aurophilic interactions on the structure-specific electronic properties leading to multi-electron redox catalysts and photoluminescence. Over the last two decades, there has been a steep rise in research related to Au^I complexes ligated by *N*-heterocyclic carbene (NHC) ligands. Compared to traditional phosphine ligands, NHC ligands have a stronger σ-donating property, and manipulation of the electronic and steric characters of NHC ligands can be more easily achieved by *N*-functionalization.

In this study, I focused on the construction of multinuclear Au^I complexes with NHC ligands. Specifically, a carbon-centered CAu^I_6 cluster and a macrocyclic dinuclear Au^I compound based on bis-NHC ligands have been developed for Au^I-based multinuclear complexes with structure-specific properties. Here, as part of my continuing study of master course, I have constructed a carbon-centered CAu^I_6 cluster with an antiprism structure. Ligand effects on structure, photochemical and redox properties are further examined. Furthermore, a helical macrocyclic dinuclear Au^I compound based on a bis-NHC ligand is constructed and the redox behaviors and luminescent properties have been clarified.

In **Chapter 2**, I describe the construction of a hexagold(I)methanium tetrafluoroborate $[C(AuI\textit{i}Pr)_6]\cdot(BF_4)_2$ by the reaction between trigold(I)oxonium salt $[O(AuI\textit{i}Pr)_3]\cdot(BF_4)$ and trimethyldiazomethane $TMSCHN_2$. Based on this, detailed characterization of the product and comparison with those of phosphine ligand supporting counterparts were conducted based on ^1H and ^{13}C NMR, ESI-TOF MS, absorption/emission, and XRD analyses in this study.

In **Chapter 3**, I describe the development of a bis-NHC ligand **L** with a pyridine-centered heterocycle-coupled spacer. In **L**, all of the heteroaromatic rings are linked by single bonds, which bring about the ready conformational flexibility. Metallation of this ligand with Au^I centers generates a macrocyclic dinuclar compounds.

Due to the flexibility and the relative position of the ligands in the macrocycle, it adapts a unique helical structure in the solid state. Also a stepwise oxidation reaction of the Au^{I} centers to synthesize dinuclear Au^{III} compound will be discussed.

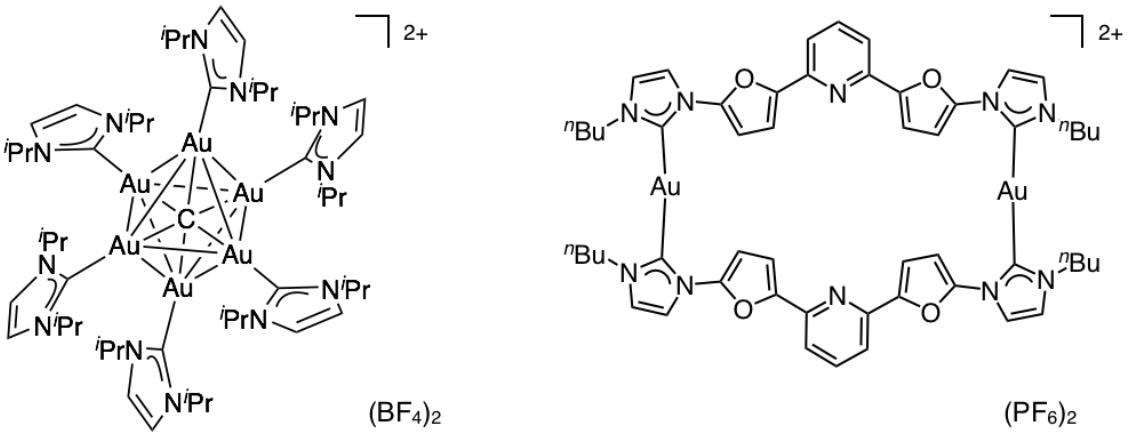

$[C(AuI\mathit{i}Pr)_6]\cdot(BF_4)_2$ $[\mathbf{L}_2Au^{I}_2]\cdot(PF_6)_2$

Figure 1-3. Molecular structures of a carbon-centered CAu^{I}_6 cluster and a macrocyclic dinuclear Au^{I} compound based on bis-NHC ligands.

1-4. References

1. G. J. Hutchings, M. Brust, H. Schmidbaur, *Chem. Soc. Rev.*, **2008**, *37*, 1759–1765.

2. H. Schmidbaur, A. Schier, *Chem. Soc. Rev.*, **2012**, *41*, 370−412.

3. H. Schmidbaur, A. Schier, *Chem. Soc. Rev.*, **2008**, *37*, 1931−1951.

4. a) R. Hoffmann, *Angew. Chem. Int. Ed. Engl.*, **1982**, *21*, 711–724; b) M. Elian, M. M. L. Chen, D. M. P. Mingos, R. Hoffmann, *Inorg. Chem.*, **1976**, *15*, 1148–1155.

5. H. G. Raubenheimer, H. Schmidbaur, *Organometallics*, **2012**, *31*, 2507–2522.

6. H. Schmidbaur, *Chem. Soc. Rev.*, **1995**, *24*, 391–400.

7. H. Schmidbaur, *Gold Bulletin*, **2000**, *33*, 3–10.

8. L. Y. Yao, T. K. Lee, V.W.W. Yam, *J. Am. Chem. Soc.*, **2016**, *138*, 7260–7263.

9. J.-H Jia, Q.-M. Wang, *J. Am. Chem. Soc.*, **2009**, *131*, 16634–16635.

10. E. E. Langdon-Jones, S. J. A. Pope, *Chem. Commun.*, **2014**, *50*, 10343–10354.

11. X. He, V. W. -W. Yam, *Coord. Chem. Rev.*, **2011**, *255*, 2111–2123.

12. X. -F. Jiang, F. K. –W.Hau, Q. -F. Sun, S. -Y. Yu, V. W. -W. Yam, *J. Am. Chem. Soc.*, **2014**, *136*, 10921–10929.

13. F. Gagosz, In *Advances in Organometallic Chemistry and Catalysis: The Silver/Gold Jubilee International Conference on Organometallic Chemistry Celebratory Book*; A. J. L. Pombeiro. Ed., pp 207.

14. V. Vreeken, D. L. J. Broere, A. C. H. Jans, M. Lankelma, J. N. H. Reek, M. A. Siegler, J. I. van. der. Vlugt, *Angew. Chem. Int. Ed.*, **2016**, *55*, 10042–10046.

15. X. -L. Pei, Y. Yang, Z. Lei, S. -S. Chang, Z. -J. Guan, X. -K. Wan, T. -B. Wen, Q. -M. Wang, *J. Am. Chem. Soc.*, **2015**, *137*, 5520–5525.

16. E. S. Smirnova, J. M. M. Molina, A. Johnson, N. A. G. Bandeira, C. Bo, A. M. Echavarren, *Angew. Chem. Int. Ed.*, **2016**, *55*, 7487–7491.

17. V. W. -W. Yam, C. -K. Li, C. -L. Chan, *Angew. Chem. Int. Ed.*, **1998**, *37*, 2857–2859.

18. T. Arif, C. Cazorla, N. Bogliotti, N. Saleh, F. Blanchard, V. Gandon, R. Métivier, J. Xie, A. Voituriez, A. Marinetti, *Catal. Sci. Technol.*, **2018**, *8*, 710–715.

19. A. J. Arduengo III, R. L. Harlow, M. Kline, *J. Am. Chem. Soc.*, **1991**, *113*, 361–363.

20. J. C. Y. Lin, R. T. W. Huang, C. S. Lee, A. Bhattacharyya, W. S. Hwang, I. J. B. Lin, *Chem. Rev.*, **2009**, *109*, 3561–3598.

21. R. H. Crabtree, *J. Organomet. Chem.*, **2005**, *690*, 5451–5457.

22. R. Visbal, A. Laguna, M. C. Gimeno, *Chem. Commun.*, **2013**, *49*, 5642–5644.
23. E. Y. Tsui, P. Müller, J. P. Sadighi, *Angew. Chem. Int. Ed.*, **2008**, *47*, 8937–8940.
24. T. J. Robilotto, J. Bacsa, T. G. Gray, J. P. Sadighi, *Angew. Chem. Int. Ed.*, **2012**, *51*, 12077–12080.
25. L. Jin, D. S. Weinberger, M. Melaimi, C. E. Moore, A. L. Rheingold, G. Bertrand, *Angew. Chem. Int. Ed.*, **2014**, *53*, 9059–9063.
26. C. E. Strasser, V. J. Catalano, *J. Am. Chem. Soc.*, **2010**, *132*, 10009–10011.
27. R. Visbal, M. C. Gimeno, *Chem. Soc. Rev.*, **2014**, *43*, 3551–3574.
28. P. F. Ai, M. Mauro, L. D. Cola, A. A. Danopoulos, P. Braunstein, *Angew. Chem. Int. Ed.*, **2016**, *55*, 3338–3341.
29. S. K. Schneider, W. A. Herrmann, E. Herdtweck, *Z. Anorg. Allg. Chem.*, **2003**, *629*, 2363–2370.
30. D. Gatineau, J. -P. Goddard, V. Mouriès-Mansuy, L. Fensterbank, *Isr. J. Chem.*, **2013**, *53*, 892–900.
31. C. F. Bender, R. A. Widenhoefer, *Org. Lett.*, **2006**, *8*, 5303–5305.

2. Carbon-centered CAu^{I}_{6} cluster

2-1. Introduction

In this chapter, I describe the construction of carbon-centered Au^I clusters supported by *N*-heterocyclic carbene ligands.

As mentioned in section **1-1**, Schmidbaur *et al.* reported a series of carbon-centered Au^I clusters in 1989. With supporting triphenyl phosphine ligands, hyper-auration takes place at a carbon center to give CAu^I_5 or even CAu^I_6 cationic clusters. These cationic clusters have attracted considerable attention, because not only of the unusual hyper-coordination of the central carbon atom, but also of the pre-determined Au–Au intramolecular contacts protected by supporting ligands. On the other hand, only very bulky phosphine ligands like tricyclohexylphosphine (PCy_3) can limit the auration reactions at the neutral tetragold(I)methane level (Figure 2-1-1).[1]

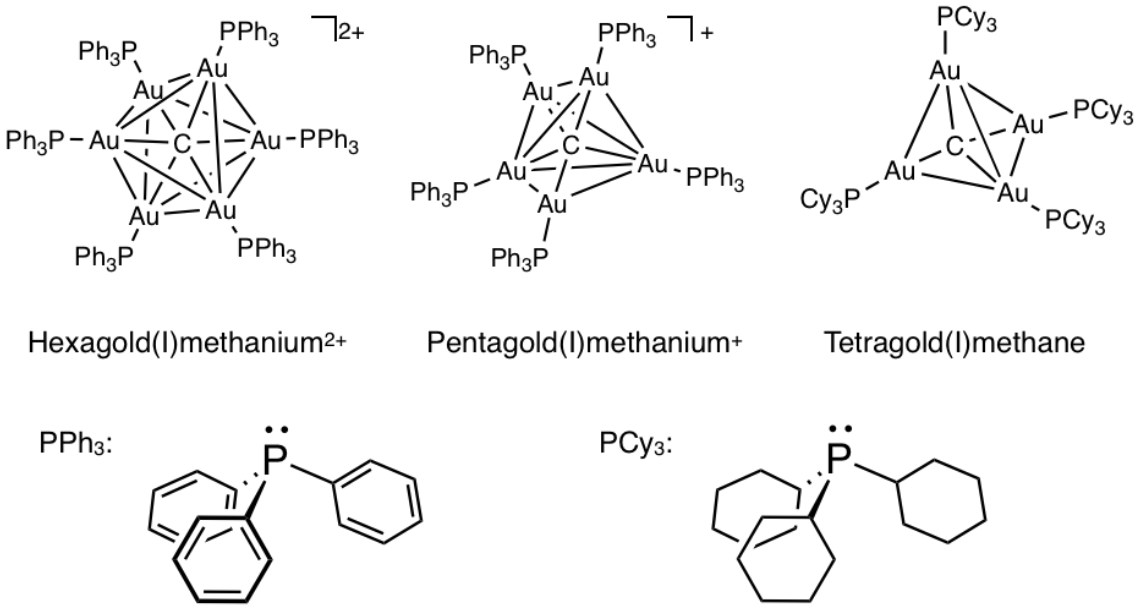

Figure 2-1-1. Carbon-centered Au^I clusters reported by Schmidbaur *et al.*

In 2009, Wang *et al.* introduced an extra metal coordination site onto an aromatic ring of a tertiary phosphine ligand to construct heterometallic $CAu^I_6Ag^I_2$ clusters, which showed luminescence even in the solution state. This was assumed to come from the structural rigidity and metallophilic interactions.[2] Later in 2014, the same group reported that a hexagold(I)methanium cluster, pre-functionalizing the supporting ligand with pyrazinyl groups, acts as a cluster linker to connect silver ions to construct a porous 3D framework.[3]

In contrast to traditional phosphine ligands, *N*-heterocyclic carbene (NHC) ligands combine strong σ-donating properties with a steric profile that allows for both stabilization of the metal center and enhancement of its catalytic activity, so that new properties were expected.

By the reaction between a trigold(I)oxonium salt $[O(AuI\textit{i}Pr)_3]\cdot(BF_4)$ and (trimethylsilyl)diazomethane ($TMSCHN_2$), a hexagold(I)methanium salt $[C(AuI\textit{i}Pr)_6]\cdot(BF_4)_2$ was obtained and successfully characterized by NMR spectroscopy, ESI-TOF MS spectrometry, and single crystal X-ray diffraction measurements. The structure and the photoluminescence properties of the $[C(AuI\textit{i}Pr)_6]\cdot(BF_4)_2$ are compared with PPh_3-supported counterparts $[C(AuPPh_3)_6]\cdot(CH_3OBF_3)_2$ and $[C(AuPPh_3)_6]\cdot(BF_4)_2$ reported by Schmidbaur *et al.*[1] in considerable detail to investigate the ligand effects on the structure-specific properties.

Constructions of carbon-centered Au^I clusters supported by two other monodentate NHC ligands: 1,3-bis(cyclohexyl)imidazol-2-ylidene (ICy) and 1,3-bis(2,4,6-trimethylphenyl)imidazol-2-ylidene (IMes) are also discussed in the last part of this chapter.

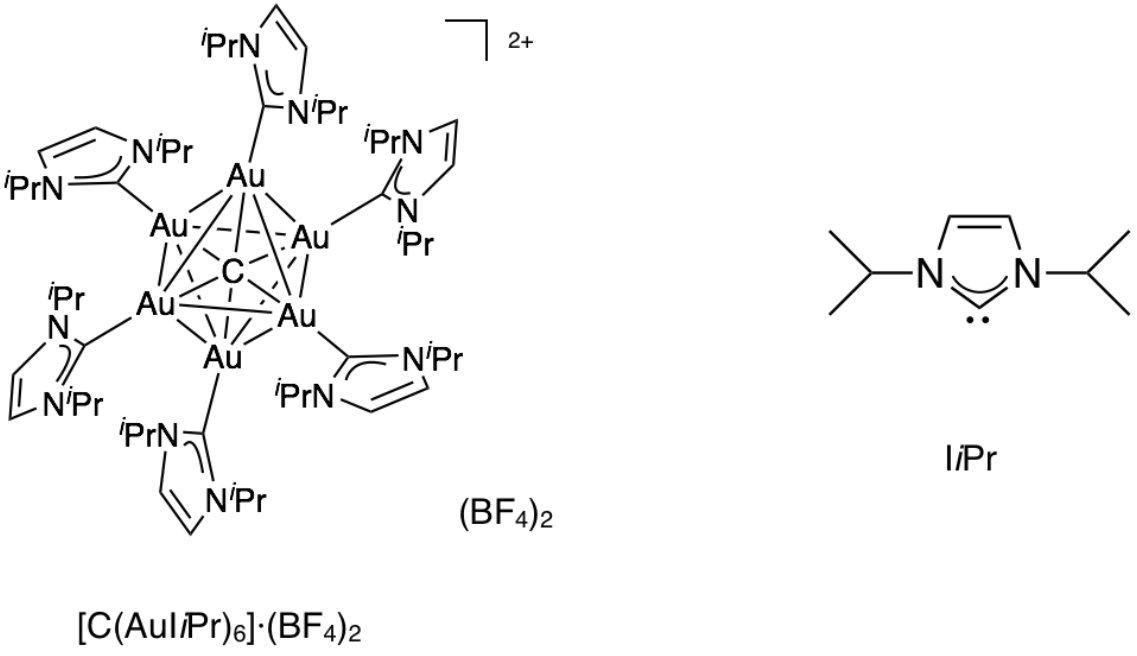

Figure 2-1-2. A key compound in this chapter: I*i*Pr-supported carbon-centered Au^I cluster, $[C(AuI\textit{i}Pr)_6]\cdot(BF_4)_2$.

2-2. Synthesis of an I*i*Pr-supported carbon-centered Au^I cluster

Schmidbaur's group reported two synthetic routes for carbon-centered Au^I clusters supported by tertiary phosphine ligands.

Firstly in 1988, for the construction of $[C(AuPPh_3)_6]\cdot(CH_3OBF_3)_2$, the synthetic method was based on the reaction of tetrakis(dimethoxyboryl)methane precursor $C[B(OCH_3)_2]_4$ as a C1 source with six Ph_3PAuCl under a basic condition (Scheme 2-2-1**)**.[1a] However, the unstable $C[B(OCH_3)_2]_4$ was not commercially available, and the synthesis required relatively harsh reaction conditions as well as a complicated purification process, which resulted in low yields.[4]

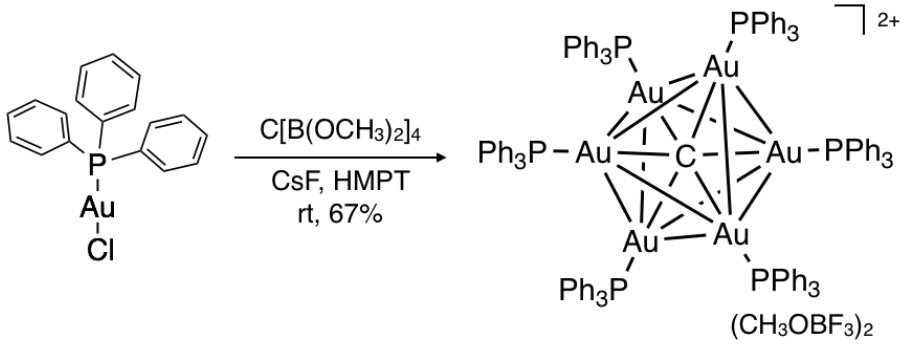

Ph_3PAuCl $[C(AuPPh_3)_6]\cdot(CH_3OBF_3)_2$

Scheme 2-2-1. Synthesis of $[C(AuPPh_3)_6]\cdot(CH_3OBF_3)_2$.

Later in 1997, the same group reported a new synthetic route for $[C(AuPPh_3)_6]\cdot(BF_4)_2$ by the reaction of (trimethylsilyl)diazomethane ($TMSCHN_2$) and tris[tripheylphosphinegold(I)]oxonium tetrafluoroborate $[O(AuPPh_3)_3]\cdot(BF_4)$ in CH_2Cl_2 in the presence of triethylamine as a base (Scheme 2-2-2).[1d]

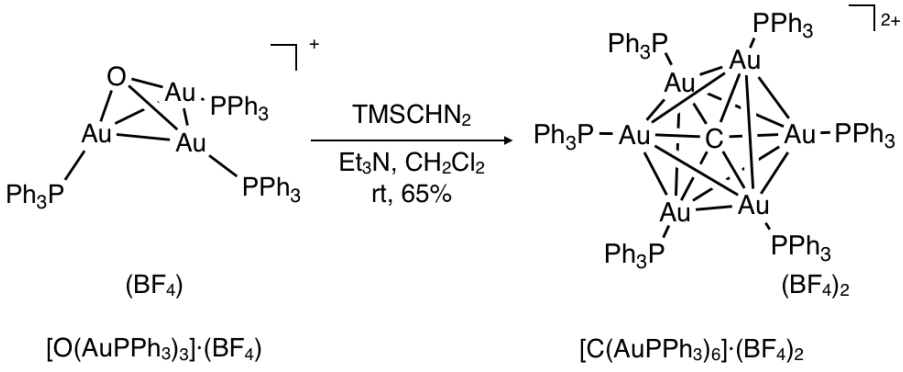

$[O(AuPPh_3)_3]\cdot(BF_4)$ $[C(AuPPh_3)_6]\cdot(BF_4)_2$

Scheme 2-2-2. Synthesis of $[C(AuPPh_3)_6]\cdot(BF_4)_2$.

The detailed synthetic route of a carbon-centered Au^{I} cluster supported by I*i*Pr ligands $[C(AuIiPr)_6]\cdot(BF_4)_2$ reported in the current work is shown in Scheme 2-2-3.

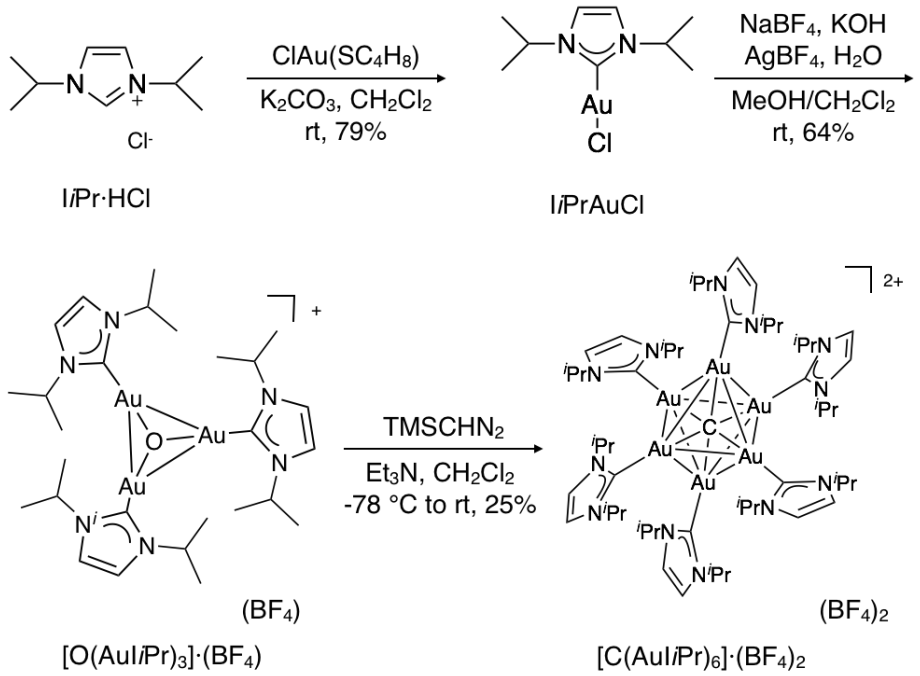

Scheme 2-2-3. Synthesis of $[C(AuIiPr)_6]\cdot(BF_4)_2$.

Firstly, I*i*PrAuCl was synthesized according to a literature-based synthetic route (Scheme 2-2-4).[5] An equimolar mixture of I*i*Pr·HCl and chloro(tetrahydrothiophene)gold(I) $ClAu(SC_4H_8)$, in CH_2Cl_2 was stirred at room temperature for 15 min, and then 20 eq. of K_2CO_3 were added. The reaction was stirred at room temperature for additional 8 h until the full consumption of the starting material $ClAu(SC_4H_8)$ was confirmed on TLC and a ^1H NMR spectrum. After removing the inorganic salts and evaporation of the solvents, I*i*PrAuCl was obtained as a colorless solid in 79% yield. This product was used without further purification.

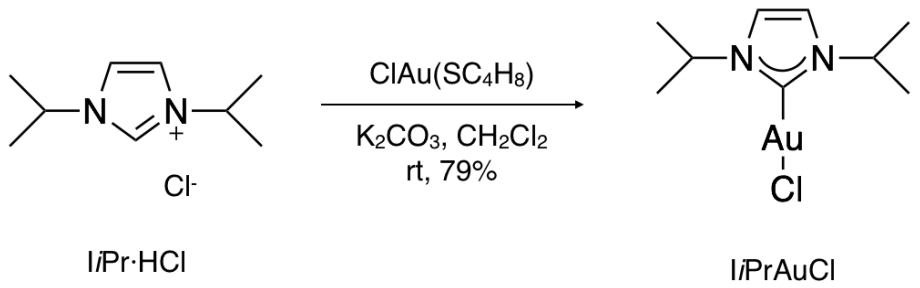

Scheme 2-2-4. Synthesis of I*i*PrAuCl.

Secondly, an I*i*Pr-supported trigold(I)oxonium salt $[O(AuI{i}Pr)_3]\cdot(BF_4)$ was prepared according to a literature-based method as shown in Scheme 2-2-5.[6] A solution of I*i*PrAuCl in CH_2Cl_2 was added to a methanol solution of KOH and $NaBF_4$. Then 1 eq. of $AgBF_4$ was added for anion exchange, followed by addition of 1 mL of water. The reaction was stirred at room temperature for 1 h until the TLC and a ^1H NMR spectrum showed the full consumption of the staring material I*i*PrAuCl. After removing the inorganic salts, reprecipitation with CH_2Cl_2/diethyl ether afforded $[O(AuI{i}Pr)_3]\cdot(BF_4)$ as a colorless solid in 64% yield.

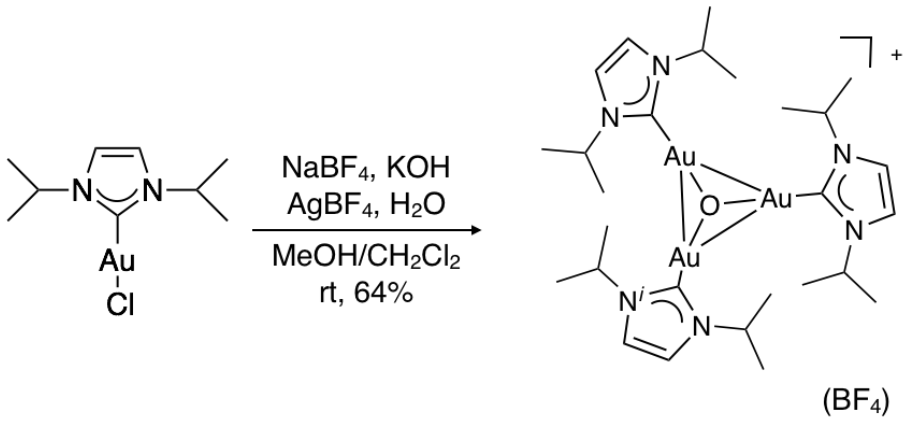

I*i*PrAuCl $[O(AuI{i}Pr)_3]\cdot(BF_4)$

Scheme 2-2-5. Synthesis of $[O(AuI{i}Pr)_3]\cdot(BF_4)$.

$[O(AuI{i}Pr)_3]\cdot(BF_4)$ was soluble in CH_2Cl_2, $CHCl_3$, acetonitrile, and methanol, but sparingly soluble in diethyl ether and *n*-hexane. $[O(AuI{i}Pr)_3]\cdot(BF_4)$ is highly stable in the solid state, whereas violet gold nano-particles appeared once dissolved in CH_2Cl_2 and stored at room temperature for 1 day, suggesting decomposition of $[O(AuI{i}Pr)_3]\cdot(BF_4)$ in solution.

The ^1H and ^{13}C NMR spectra in $CDCl_3$ of $[O(AuI{i}Pr)_3]\cdot(BF_4)$ showed only one set of signals for the I*i*Pr ligand, indicating its high symmetrical structure in solution (Figures 2-2-1 and 2-2-2.). Its ^1H NMR spectrum stayed almost unchanged when compared with that of starting material I*i*PrAuCl. On the other hand, its ^{13}C NMR spectrum showed a $C_{carbene}$ signal at 159.9 ppm, which was shifted upfield by 9 ppm (I*i*PrAuCl: $C_{carbene}$ = 168.7 ppm), indicating the decreased electron donation from I*i*Pr ligand to the Au^I center.

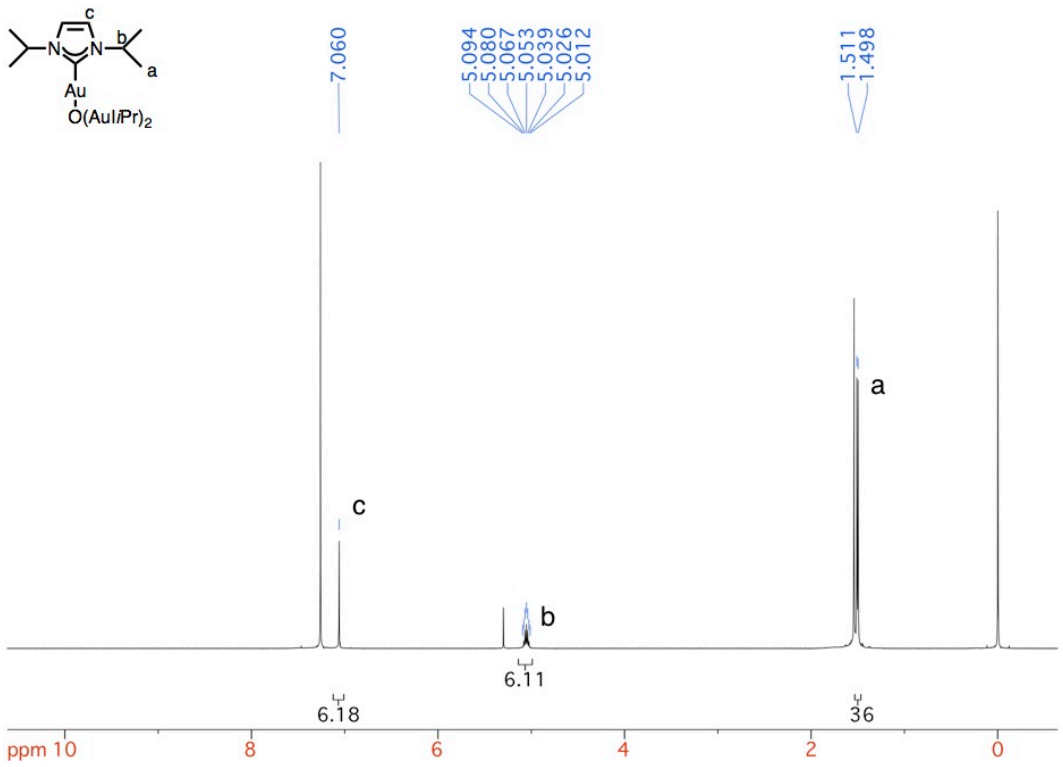

Figure 2-2-1. A ^{1}H NMR spectrum of [O(Au*i*Pr)$_3$]·(BF$_4$) (500 MHz, 300 K, CDCl$_3$).

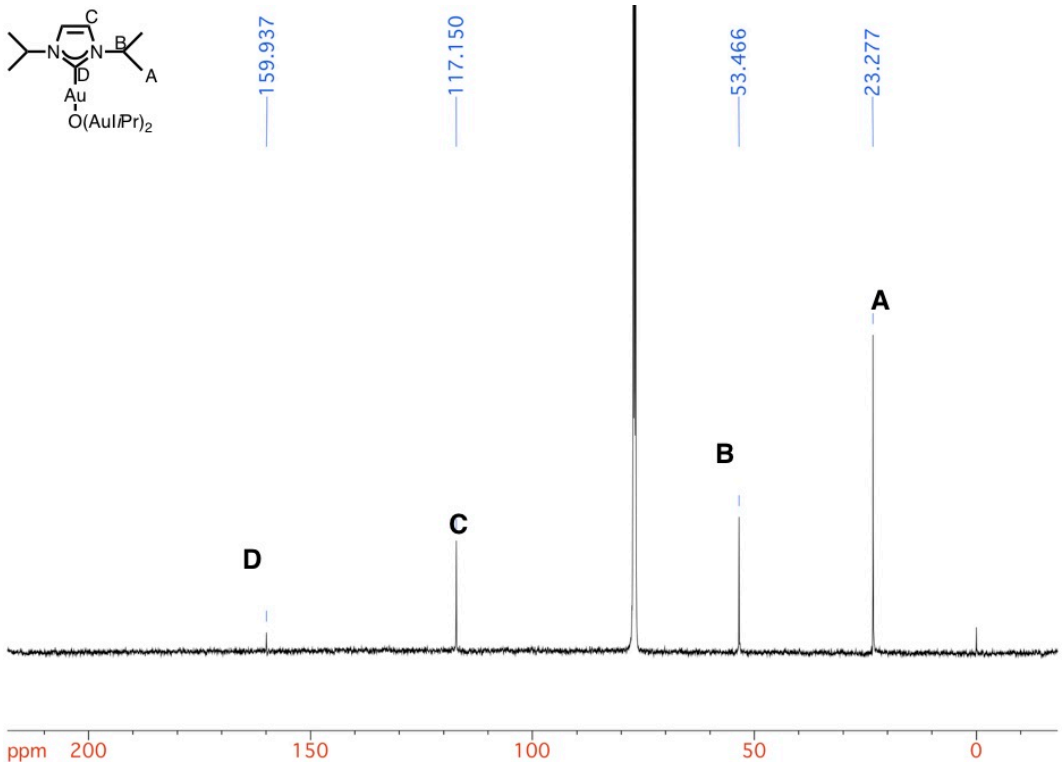

Figure 2-2-2. A ^{13}C NMR spectrum of [O(Au*i*Pr)$_3$]·(BF$_4$) (126 MHz, 300 K, CDCl$_3$).

An intense signal of the $[O(AuI\textit{i}Pr)_3]^+$ cation was observed in the ESI-TOF MS spectrum at m/z = 1063.3 (Figure 2-2-3). This result suggests that the $[O(AuI\textit{i}Pr)_3]^+$ cation is chemically stable in solution under ambient conditions.

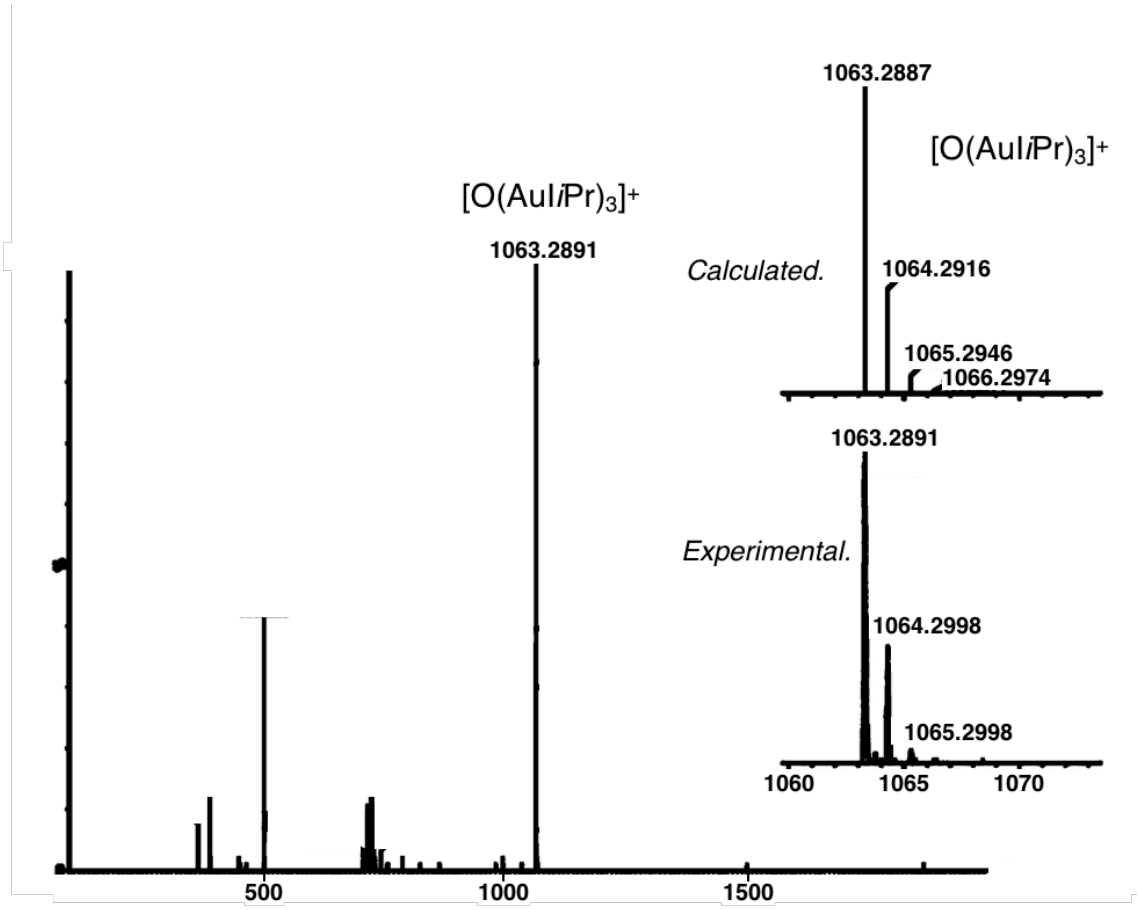

Figure 2-2-3. An ESI-TOF MS spectrum of $[O(AuI\textit{i}Pr)_3]\cdot(BF_4)$ (positive, CH_3CN, Capillary: 200 V; Sample cone: 0 V).

Single crystals of $[O(AuI\textit{i}Pr)_3]\cdot(BF_4)$ were obtained as colorless block crystals by slow evaporation of its mixed CH_2Cl_2/diethyl ether solution. The crystals are triclinic, and the X-ray crystallographic data showed that the space group is *P*-1 and each unit cell includes four $[O(AuI\textit{i}Pr)_3]^+$ cations, four BF_4^- ions, and two CH_2Cl_2 molecules.

The molecular structure of $[O(AuI\textit{i}Pr)_3]\cdot(BF_4)$ clearly showed that an OAu^I_3 tetrahedron core are bound by three I*i*Pr ligands, and that the two $[O(AuI\textit{i}Pr)_3]^+$ cations undergo intermolecular aggregation to form a centro-symmetric dimer due to the intermolecular aurophilicity (Figure 2-2-4). This kind of aggregation was also observed with phosphine supported $[O(AuPR_3)_3]^+$ clusters.[7]

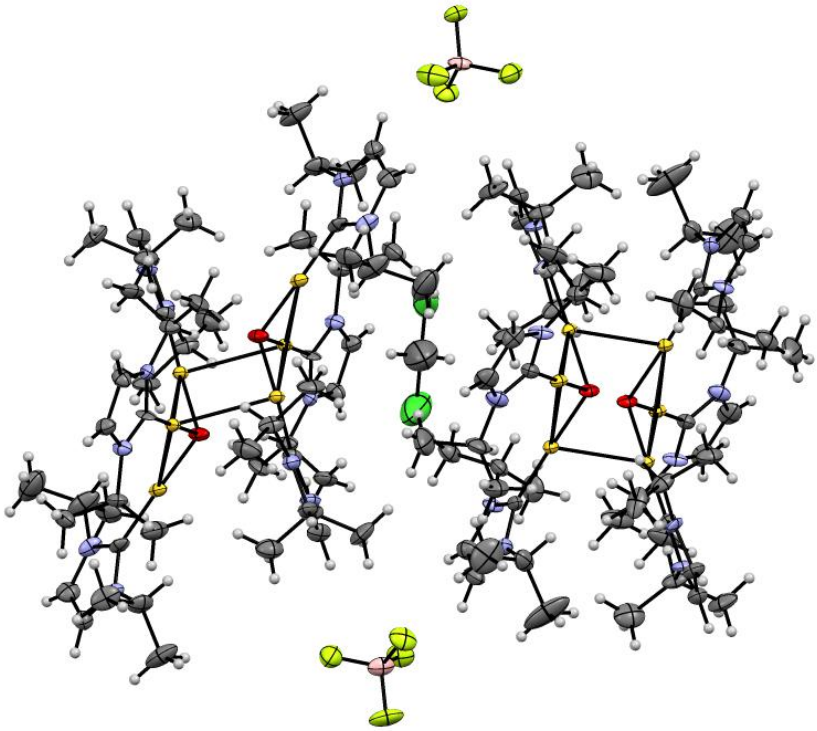

Figure 2-2-4. Single crystal X-ray structure of $[O(AuI\textit{i}Pr)_3]\cdot(BF_4)\cdot 0.5CH_2Cl_2$ with 50% probability.

Whereas the single crystal structure of $[O(AuI\textit{i}Pr)_3]\cdot(BF_4)$ shows a centro-symmetric dimeric structure, the observations that its ^1H NMR spectrum shows only one set of signals of I*i*Pr ligands as well as its ESI-TOF MS spectrum shows an intense signal of $[O(AuI\textit{i}Pr)_3]^+$ cation, indicate that $[O(AuI\textit{i}Pr)_3]\cdot(BF_4)$ exists as a monomer in solution.

Finally, an 1,3-bis(isopropyl)imidazol-2-ylidene (I*i*Pr)–supported carbon-centered Au^I cluster, $[C(AuI\textit{i}Pr)_6]\cdot(BF_4)_2$, was synthesized by the reaction of $[O(AuI\textit{i}Pr)_3]\cdot(BF_4)$ with trimethylsilyldiazomethane ($TMSCHN_2$) in the presence of triethylamine in CH_2Cl_2.[1d] After reprecipitation in CH_3CN/diethyl ether several times, $[C(AuI\textit{i}Pr)_6]\cdot(BF_4)_2$ was obtained as a brown solid in 25% yield, which is stable toward oxygen, moisture, heat, and light. The formation of byproduct $[Au(I\textit{i}Pr)_2]^+$ species as well as the loss during the purification steps may have resulted in the low yield.

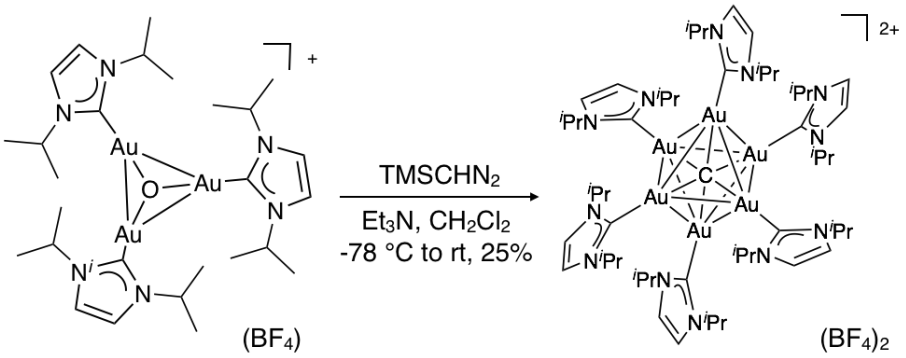

Scheme 2-2-6. Synthesis of $[C(AuI\mathit{i}Pr)_6]\cdot(BF_4)_2$.

^{1}H and ^{13}C NMR spectra of $[C(AuI\mathit{i}Pr)_6]\cdot(BF_4)_2$ are shown in Figure 2-2-5 and Figure 2-2-6, respectively. At room temperature, only one set of signals of I*i*Pr ligands was observed in the ^{1}H and ^{13}C NMR spectrum in CD_3CN, showing its highly symmetrical structure in solution. This observation suggests that there is free rotation about the C–Au bonds at room temperature in solution. The ^{13}C NMR signal corresponding to the $C_{carbene}$ appeared at 182.3 ppm in CD_3CN, while that of the central carbon was not detected. Schmidbaur *et al.* reported that a ^{13}C NMR signal of $CAu_6(PR_3)_6$ appeared at 137 ppm in CD_2Cl_2, using ^{13}C-labeled CCl_4 as a C1 source to enhance the intensity of the signal because it showed a P-coupled septet signal[8]. In the current work no signals corresponding to the central carbon atom were observed around 140 ppm. In this case, two possible reasons for the absence of the signal of the central carbon are assumed. One possible reason is that the intensity of the signal was too weak due to the long or short T_1 value specific to the CAu_6 structure. If the carbon has a very long T_1 relaxation time, the signal should become broadened. On the other hand, in the case the T_1 relaxation time is too short, the signal may be weakened during the measurements. The other possible reason is the chemical shift of the signal is out of range.

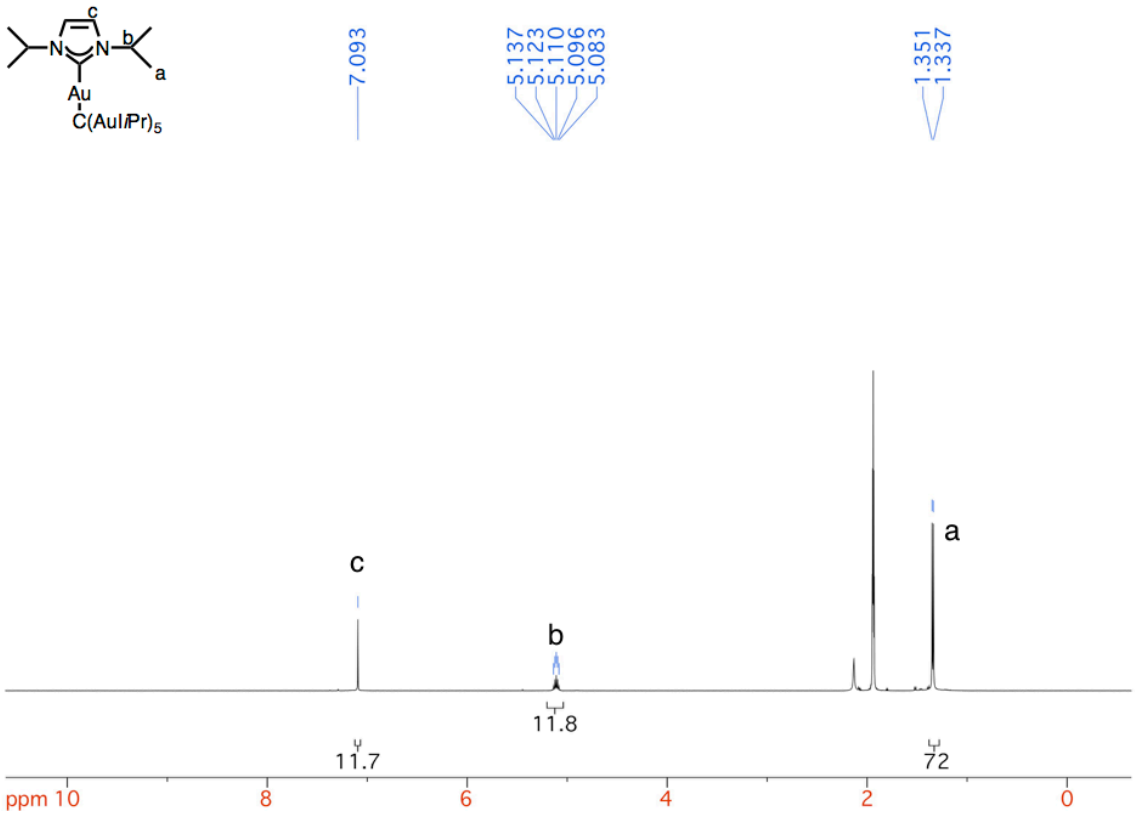

Figure 2-2-5. A ^{1}H NMR spectrum of $[C(AuI\mathit{i}Pr)_6]\cdot(BF_4)_2$ (500 MHz, 300 K, CD_3CN).

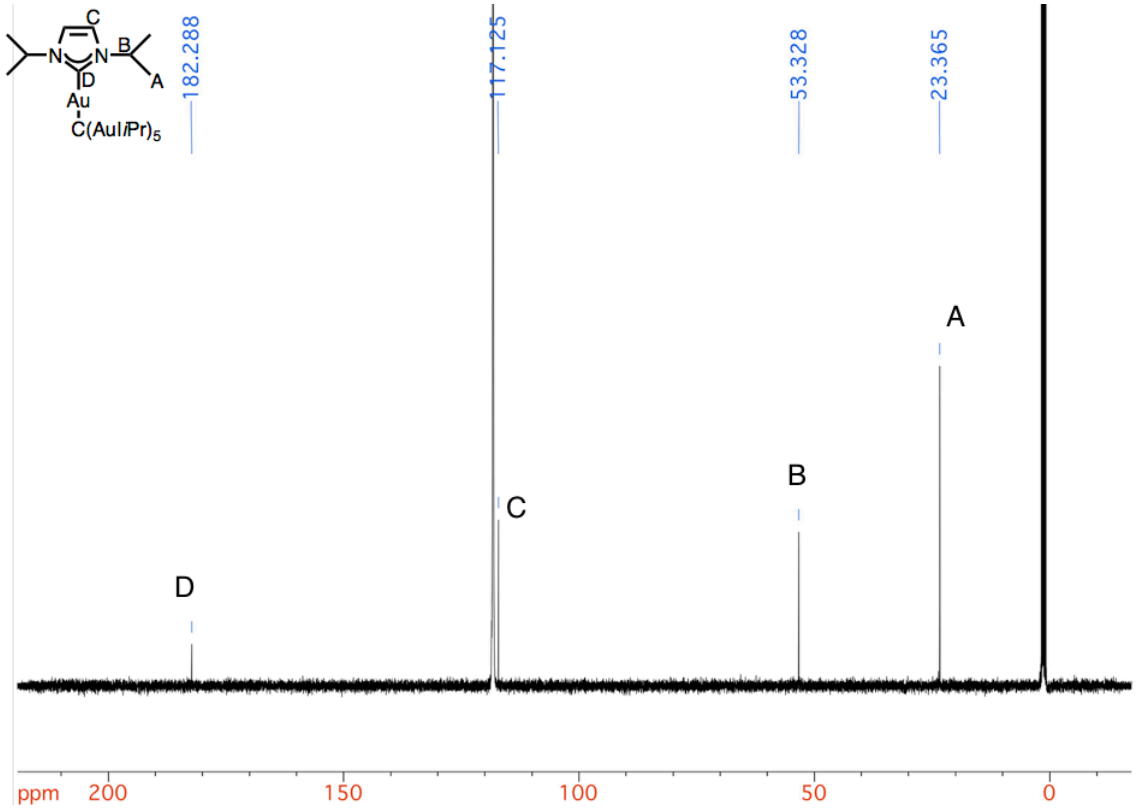

Figure 2-2-6. A ^{13}C NMR spectrum of $[C(AuI\mathit{i}Pr)_6]\cdot(BF_4)_2$ (126 MHz, 300 K, CD_3CN).

It would be interesting to see if there is any temperature-dependence of these signals of I*i*Pr ligands and a possible splitting owing to the congestion at the cluster surface of $[C(AuI\textit{i}Pr)_6]\cdot(BF_4)_2$. Therefore, ^{1}H NMR measurement in acetonitrile-d_3 was conducted at 250 K. Comparing the ^{1}H NMR spectrum taken at 250 K with that taken at 300 K, neither temperature-dependence nor splitting of the signals was observed even at 250 K (Figure 2-2-7). The free rotation about the C–Au bonds seems to be possible even at low temperatures.

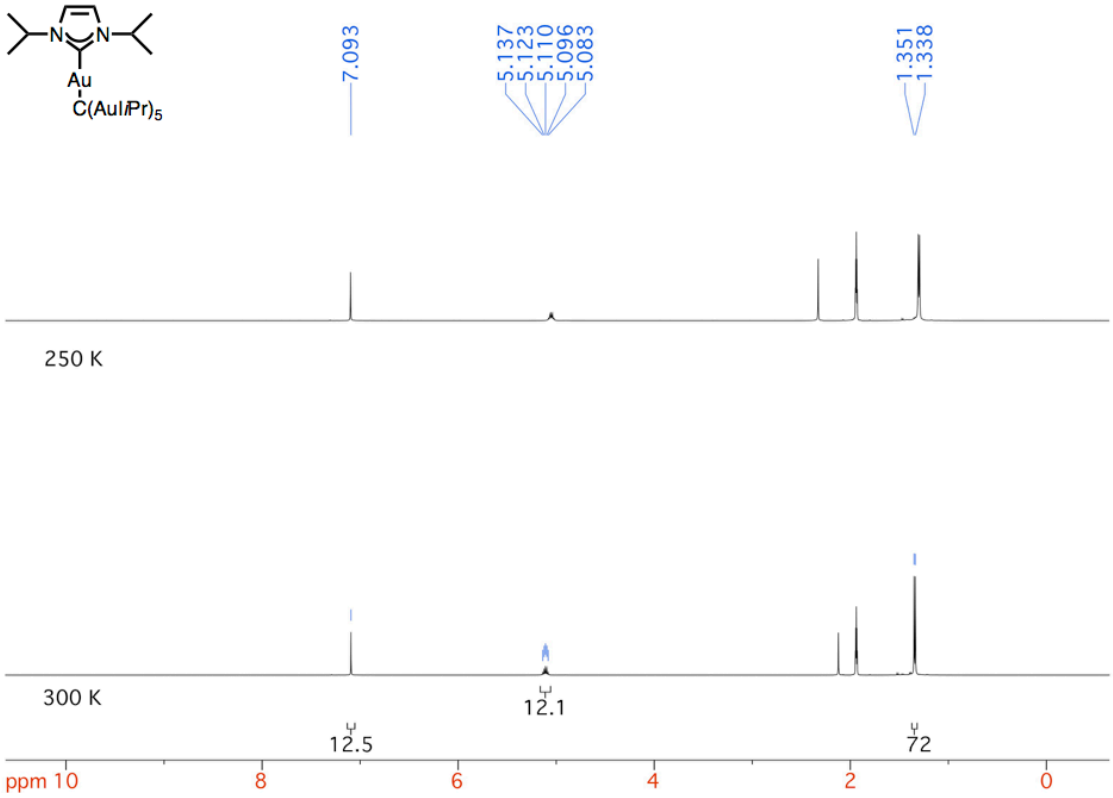

Figure 2-2-7. A comparison of NMR spectra of $[C(AuI\textit{i}Pr)_6]\cdot(BF_4)_2$ at 300 K and 250 K (500 MHz, CD_3CN).

In an ESI-TOF MS spectrum of $[C(AuI\textit{i}Pr)_6]\cdot(BF_4)_2$, the signal of dication $[C(AuI\textit{i}Pr)_6]^{2+}$ was detected as an intense peak appeared at m/z = 1053.3, which suggests that $[C(AuI\textit{i}Pr)_6]^{2+}$ is chemically stable in solution under ambient conditions (Figure 2-2-8).

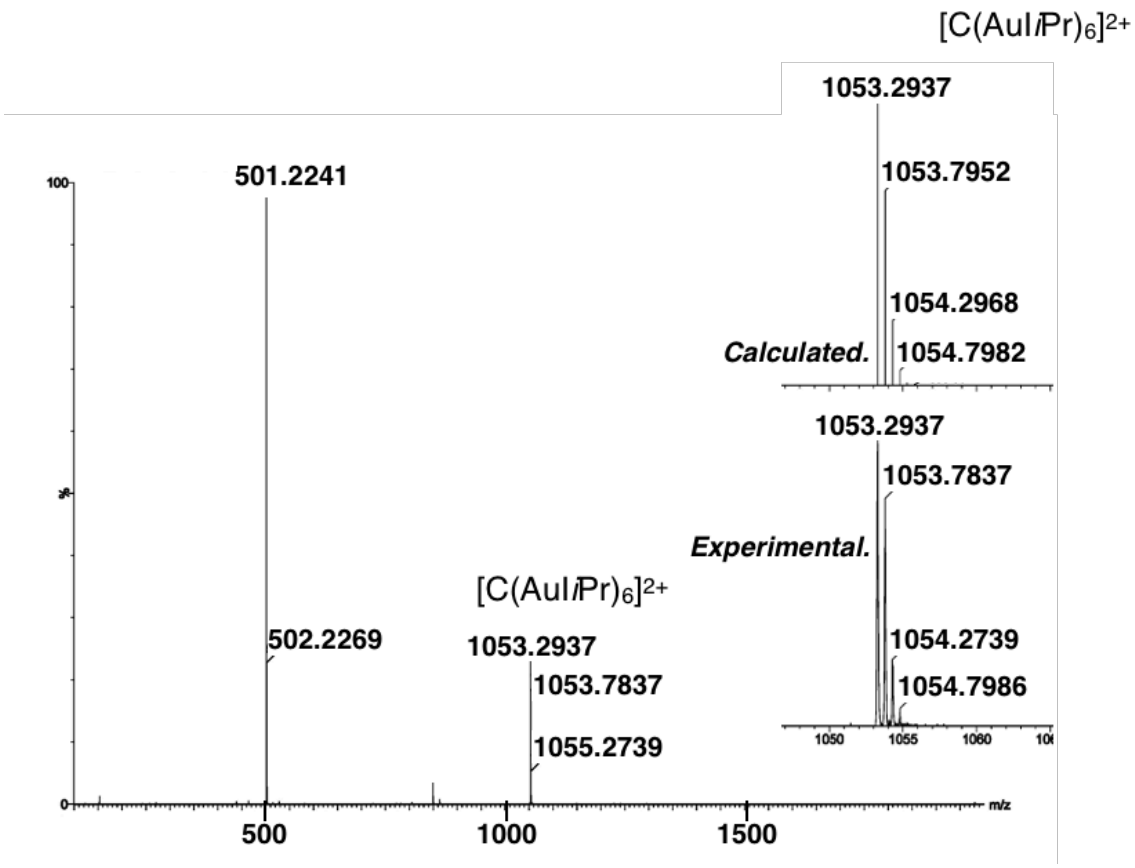

Figure 2-2-8. An ESI-TOF MS spectrum of $[C(AuI\mathit{i}Pr)_6]^{2+}$ (positive, CH_3CN, Capillary: 3000 V; Sample cone: 30 V).

A single crystal of $[C(AuI\mathit{i}Pr)_6]\cdot(BF_4)_2$ suitable for an XRD measurement was obtained as a yellow block crystal by slow evaporation from its mixed CH_2Cl_2/*n*-hexane solution at room temperature (Figures 2-2-9 and 2-2-10). The crystals are trigonal, and the X-ray crystallographic data showed that the space group is *P*-3 and each unit cell includes one $[C(AuI\mathit{i}Pr)_6]^{2+}$ dication and two BF_4^- anions. The lattice is built up of independent dications and anions without any unusual sub-van der Waals contacts between these components. The $[C(AuI\mathit{i}Pr)_6]\cdot(BF_4)_2$ cluster has an antiprism structure with D_{3h} symmetry.

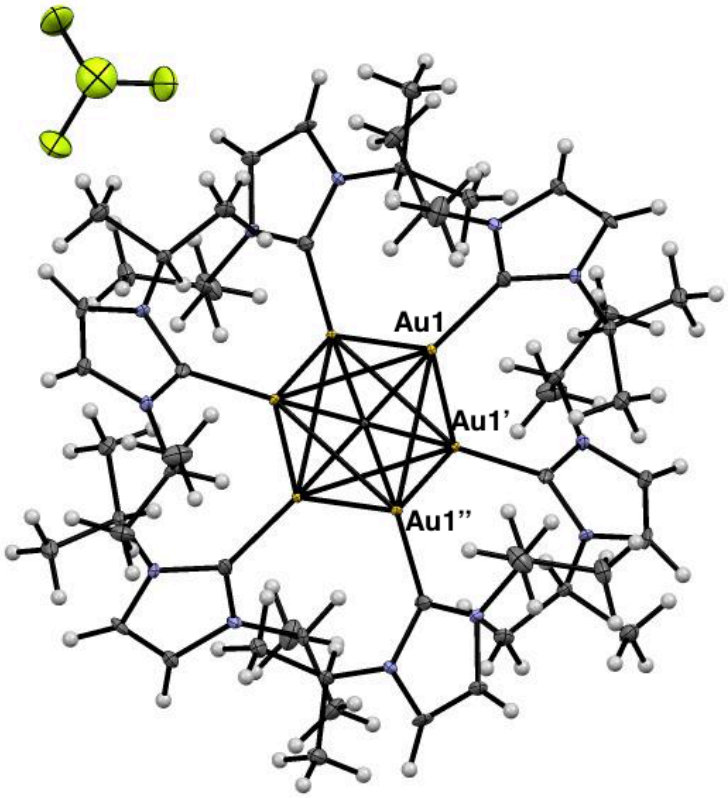

Figure 2-2-9. ORTEP diagram of $[C(AuI\mathit{i}Pr)_6]\cdot(BF_4)_2$ with 50% probability.

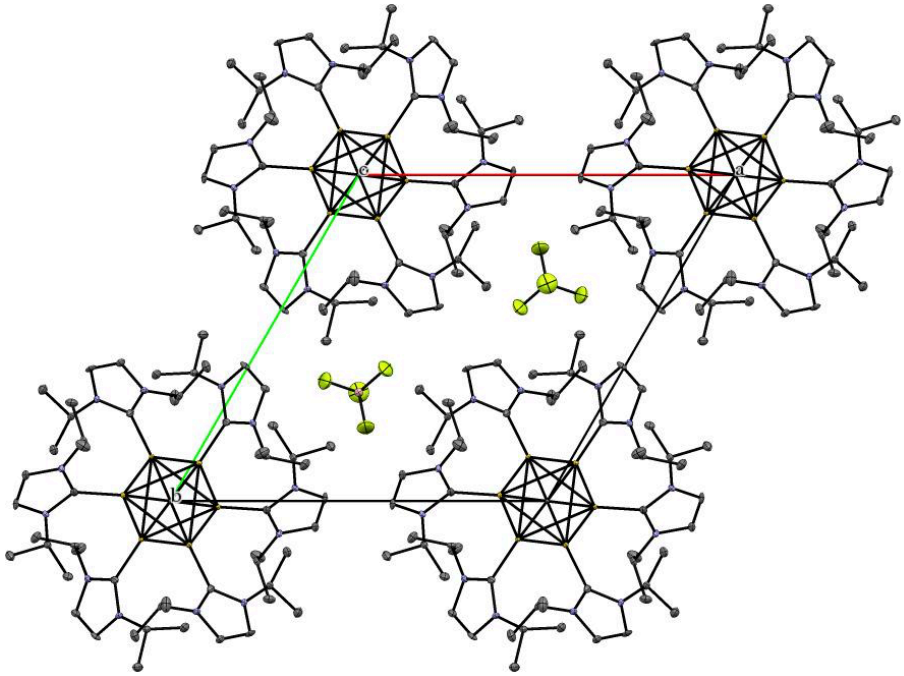

Figure 2-2-10. A unit cell contains one $[C(AuI\mathit{i}Pr)_6]^{2+}$ dication and two BF_4^- anions without any solvent molecules (H atoms are omitted for clarity).

An I*i*Pr ligand binds to each gold atom so as to keep the Au^I center and one carbene carbon atom aligned with the central carbon atom. The Au–$C_{carbene}$ bonds are a little longer than those of other NHC–Au complexes reported so far, which may be a result of the structure distortion to accommodate six I*i*Pr ligands around the CAu^I_6 core.

The bond distances of Au1–Au1' and Au1'–Au1'' are 3.0548(3) Å and 2.9282(3) Å, respectively. This result suggests strong intramolecular Au–Au interactions in the cluster.[9] In spite of the fact that all the Au^I atoms are crystallographically equivalent, its structure has relatively low symmetry, which may come from the packing force or bulky I*i*Pr ligands. Some selected bond lengths and angles are shown in Tables 2-1 and 2-2.

Table 2-1. Selected bond lengths (Å)

Au1	Au1'	3.0548(3)
Au1	Au1''	2.9282(3)
Au1	C1	2.1158(3)
Au1	C2	2.021(6)

Table 2-2. Selected angles (°)

Au1	C1	Au1'	92.424(9)
Au1	C1	Au1''	87.576(9)
C1	Au1	C2	173.06(16)

2-3. Comparison of I*i*Pr-supported and PPh_3-supported CAu^I_6 clusters

The I*i*Pr-supported carbon-centered Au^I cluster prepared in this study was compared with the PPh_3-supported counterparts $[C(AuPPh_3)_6]\cdot(CH_3OBF_3)_2$ and $[C(AuPPh_3)_6]\cdot(BF_4)_2$, previously reported by Schmidbaur *et al.* in 1988[1a] and 1997[1d], respectively. As a result, significant ligand effects on structure-specific properties were observed, mainly concerning their crystal structures and photoluminescence behaviors.

At first, the crystal structure of the $[C(AuI\textit{i}Pr)_6]\cdot(BF_4)_2$ was compared with $[C(AuPPh_3)_6]\cdot(CH_3OBF_3)_2$ as well as $[C(AuPPh_3)_6]\cdot(BF_4)_2$ in detail as shown in Table 2-3.

Table 2-3. Comparison of three carbon-centered Au^I clusters.

	$[C(AuI\textit{i}Pr)_6]\cdot(BF_4)_2$	**$[C(AuPPh_3)_6]\cdot(BF_4)_2$**	**$[C(AuPPh_3)_6]\cdot(CH_3OBF_3)_2$**
Symmetry	trigonal, space group *P*-3 D_{3h}	monoclinic, space group $P2_1/c$, no crystallographically imposed symmetry	monoclinic, space group $P2_1/c$, a center of inversion
Au-Au distance (Å)	2.9282(3), 3.0548(3)	2.887(1)–3.226(1)	2.910(1)–3.053(1)
Au-C distance (Å)	2.1158(3)	2.09(1)–2.15(1)	2.122(2)–2.129(2)
Au-L distance (Å)	2.021(6)	2.254(4)–2.277(4)	2.269(2)–2.274(3)

- *Similarities*

All of these three clusters show a CAu^I_6 core structure supported by six supporting ligands (I*i*Pr or PPh_3), with a sublinear coordination geometry on the Au^I centers.

The Au–Au distances are comparable for $[C(AuI\textit{i}Pr)_6]\cdot(BF_4)_2$ (2.9282(3) and 3.0548(3) Å) to PPh_3-supported carbon-centered Au^I clusters (2.887(1)–3.226(1) Å for $[C(AuPPh_3)_6]\cdot(BF_4)_2$, 2.910(1)–3.053(1) Å for $[C(AuPPh_3)_6]\cdot(CH_3OBF_3)_2$). These short distances indicate strong intramolecular Au–Au interactions in all these compounds.

The bond distances between the central carbon and an Au^I atom are also comparable to those of $[C(AuI\textit{i}Pr)_6]\cdot(BF_4)_2$ (2.1158(3) Å) and PPh_3-supported carbon-centered Au^I clusters (2.09(1)–2.15(1) Å for $[C(AuPPh_3)_6]\cdot(BF_4)_2$, 2.122(2)–2.129(2) Å for $[C(AuPPh_3)_6]\cdot(CH_3OBF_3)_2$), which are significantly longer compared to those of general C–Au bonds. This longer distance most likely comes from the larger coordination number on the central carbon as well as the steric hindrance between the adjacent supporting ligands.

- *Differences*

The most significant difference among these three clusters is their crystallographic symmetry. The $[C(AuI\textit{i}Pr)_6]\cdot(BF_4)_2$ complex analyzed in this work shows an antiprism structure with D_{3h} symmetry. The phosphine-supported counterpart $[C(AuPPh_3)_6]\cdot(CH_3OBF_3)_2$ reported by Schmidbaur *et al.* in 1988 showed a lower symmetry, as a distorted octahedral CAu^I_6 structure with conversion center occupied by the central carbon atom. On the other hand, the $[C(AuPPh_3)_6]\cdot(BF_4)_2$ complex reported later in 1997, bearing the same counter anion as the current work (BF_4^-), showed a distorted octahedron structure in which no crystallography symmetries were observed. This result indicates that, with larger triphenylphosphine ligands, the CAu^I_6 core required to distort from an ideal octahedron structure in order to accommodate all the six ligands, which resulted in less or even no crystallographic symmetry. On the other hand, the smaller I*i*Pr ligands distorted the carbon-centered clusters to a much less extent.

Last but not least, the I*i*Pr ligands occupy a position closer to the CAu^I_6 core with a much shorter metal–ligand distance (Au–$C_{carbene}$ 2.021(6) Å) compared with Au–PPh_3 distances (Au–P 2.254(4)–2.277(4) Å for $[C(AuPPh_3)_6]\cdot(BF_4)_2$ and 2.269(2)–2.274(3) Å for $[C(AuPPh_3)_6]\cdot(CH_3OBF_3)_2$).

In addition, the photoluminescence properties of the $[C(AuI\mathit{i}Pr)_6]\cdot(BF_4)_2$ and PPh_3-supported carbon-centered Au^I clusters were also compared.

The photoluminescence measurement of $[C(AuI\mathit{i}Pr)_6]\cdot(BF_4)_2$ in the solid state revealed that it is luminescent with yellow-green emission under UV irradiation at λ_{em}^{max} 547 nm (Figure 2-3-2). However, as the pictures shown in Figure 2-3-2, in spite of the luminescence observed by naked eyes, the quantum yield of the emission was too low to measure.

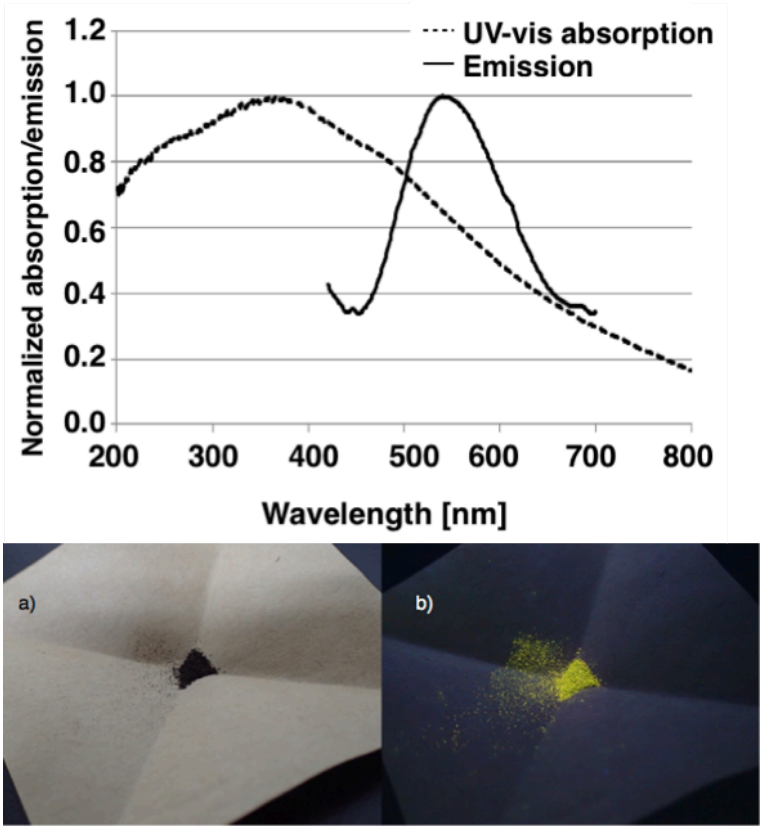

Figure 2-3-2. UV-vis absorption and emission spectra of $[C(AuI\mathit{i}Pr)_6]\cdot(BF_4)_2$ in the solid state at 293 K. Pictures of $[C(AuI\mathit{i}Pr)_6]\cdot(BF_4)_2$ in the solid state at room temperature: a) under natural light and b) under irradiation by UV lamp (365 nm).

The photochemical behaviors of $[C(AuI\mathit{i}Pr)_6]\cdot(BF_4)_2$ are very similar to those of the phosphine-supported counterpart $[C(AuPPh_3)_6]\cdot(BF_4)_2$ which exhibits green emission at λ_{em}^{max} 537 nm at room temperature, as reported by Wang *et al.* in 2009.[2] It is noteworthy that the $[C(AuI\mathit{i}Pr)_6]\cdot(BF_4)_2$ complex has a longer wavelength emission (λ_{em}^{max} 544 nm) compared to the PPh_3-supported $[C(AuPPh_3)_6]\cdot(BF_4)_2$. This result agrees with the observation that emission energy correlates inversely to the Au–Au distances.[10] This difference may come from the strong σ-coordination ability of NHC ligands compared to phosphine ligands. Also, the luminescence of these gold clusters is presumed to be phosphorescent in nature. It is noteworthy that for all of the carbon-centered Au^I clusters, the emission was too weak in solution at room temperature. In solution, the photo-excited state of the carbon-centered Au^I clusters may relax through radiationless processes, for instance, the free rotation of ligands. Schmidbaur *et al.*[1a] reported that the bonds between the central carbon atom and the six Au^I atoms come from the six sp hybride orbitals of the Au atoms and the s and p orbitals of the central C atom. Later Wang *et al.* reported the nature of the emission for CAu^I_6 was tentatively assigned to a cluster-based metal-centered excited state, and excited electron could be transferred from CAu_6 core to the surrounding ligands with a large HOMO–LUMO gap. Further study concerning the luminescence behaviors of the carbon-centered Au^I clusters will be conducted at lower temperature.

As a result of the comparison of these three carbon-centered Au^I clusters supported by different ligands, it is obvious that they share many things in common. However, the electronic and steric factors resulting from the ligands significantly affect their electronic properties. Further study of the ligand effect and the influences of aurophilic interactions on the CAu^I_6 clusters will focus on their specific photoluminescence properties, for instance, lifetime and quantum yield of the emission, as well as on the central carbon center.

2.4 Carbon-centered Au^I clusters supported by other NHC ligands

To further investigate the ligand effects on the structure-specific properties and to achieve effective control of the coordination number of the central carbon atom by taking advantage of the steric properties of supporting ligands, carbon-centered Au^I clusters supported by two other monodentate NHC ligands: 1,3-bis(2,4,6-methylphenyl)imidazol-2-ylidene (IMes) and 1,3-bis(cyclohexyl)imidazol-2-ylidene (ICy) were also examined.

In 1992, Schmidbaur *et al.* have reported a neutral tetragold(I)methane complex $C(AuPCy_3)_4$ and proposed that this complex should have a tetrahedron structure (Scheme 2-4-1).[1c] However, this assumption has not been confirmed because its single crystal structure is sill missing. The failure in crystalizing $C(AuPCy_3)_4$ may come from the extended Au–Au distance in the $C(AuPCy_3)_4$ tetrahedron core and therefore from the destabilization due to the decrease in aurophilicity.

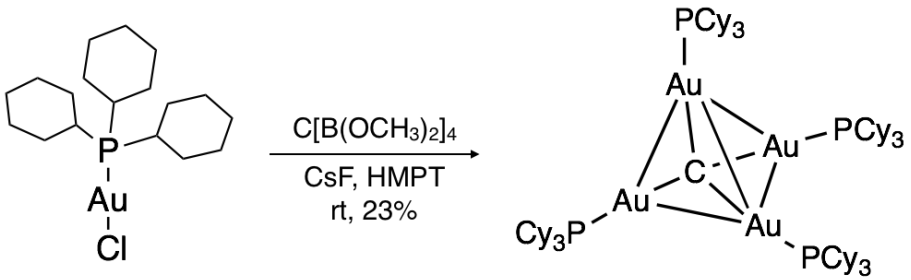

PCy_3AuCl $C(AuPCy_3)_4$

Scheme 2-4-1. Synthesis of $C(AuPCy_3)_4$.

In order to construct tetragold(I)methane $C(AuNHC)_4$ species, 1,3-bis(2,4,6-trimethylphenyl)imidazol-2-ylidene (IMes) bearing two bulky mesityl substituents was chosen as a candidate. A trigold(I)oxonium salt $[O(AuIMes)_3]\cdot(BF_4)$ supported by IMes ligands was synthesized according to literature-based procedures.[6] The reaction between the trigold(I)oxonium salt $[O(AuIMes)_3]\cdot(BF_4)$ with trimethylsilyldiazomethane ($TMSCHN_2$) was conducted several times, however, no carbon-centered Au^I clusters were detected by ESI-TOF MS spectrometry (Scheme 2-4-2 and Figure 2-4-1). The steric hindrance between adjacent IMes ligands seems to hinder the generation of $C(AuIMes)_4$.

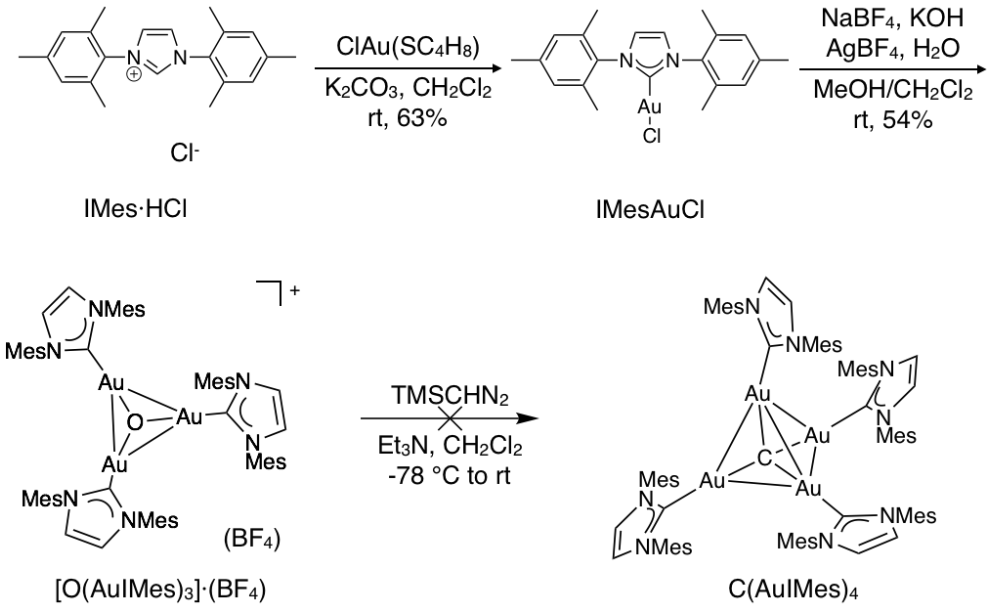

Scheme 2-4-2. A synthetic approach to $C(AuIMes)_4$.

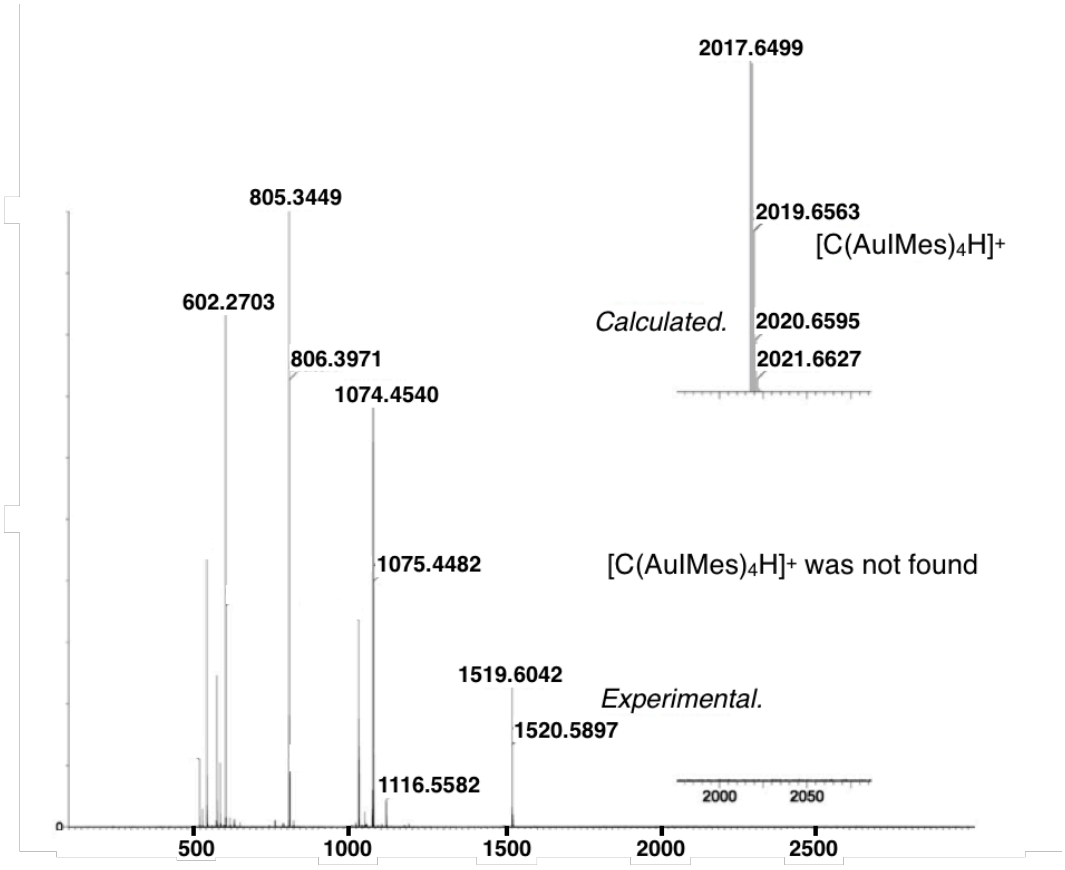

Figure 2-4-1. An ESI-TOF MS spectrum for the reaction between $[O(AuIMes)_3]\cdot(BF_4)$ and $TMSCHN_2$ (positive, CH_3CN, Capillary: 3000 V; Sample cone: 30 V).

Finally, the construction of carbon-centered Au^I clusters supported by 1,3-bis(cyclohexyl)imidazol-2-ylidene (ICy) ligands was conducted by the reaction between a trigold(I)oxonium salt $[O(AuICy)_3]\cdot(BF_4)$ and trimethylsilyldiazomethane $TMSCHN_2$ (Scheme 2-4-3). The trigold(I)oxonium salt $[O(AuICy)_3]\cdot(BF_4)$ was synthesized according to a literature-based procedure.[6] Then the reaction between trigold(I)oxonium salt $[O(AuICy)_3]\cdot(BF_4)$ and $TMSCHN_2$ was conducted and monitored by ESI-TOF MS spectrometry. As a result, an ICy-supported $[C(AuICy)_6]^{2+}$ dication was detected as a weak signal in the complicated ESI-TOF MS spectrum at *m/z* = 1293.4 (Figure 2-4-2). On the other hand, in a ^1H NMR spectrum of the reaction product, most signals were broadened and overlapped with each other, which may be due to the instability of the resulting carbon-centered Au^I cluster (Figure 2-4-3).

Furthermore, single crystals of $[C(AuICy)_6]\cdot(BF_4)_2$ were obtained by slow evaporation of a mixed CH_2Cl_2/*n*-hexane solution at room temperature as yellow block crystals. Single-crystal X-ray diffraction analysis also revealed a CAu^I_6 structure, however, the crystal structure could not be fully solved because the ligand structures were terribly disordered, presumably due to the congestion at the cluster surface. Further trials for isolation and characterization of $[C(AuICy)_6]\cdot(BF_4)_2$ are now under way.

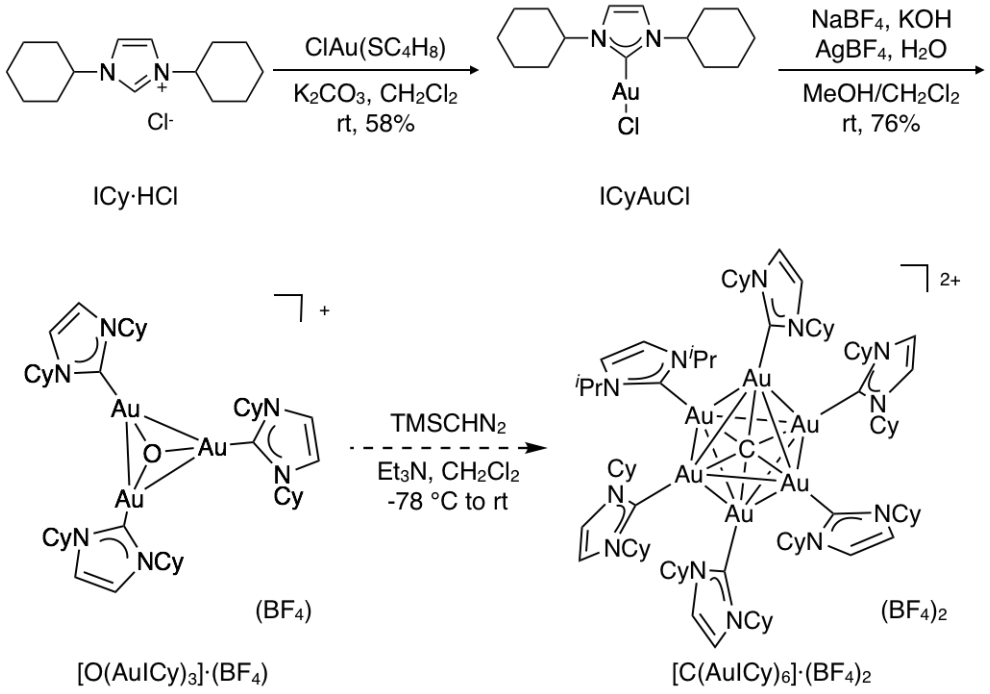

Scheme 2-4-3. A synthetic approach to $[C(AuICy)_6]\cdot(BF_4)_2$.

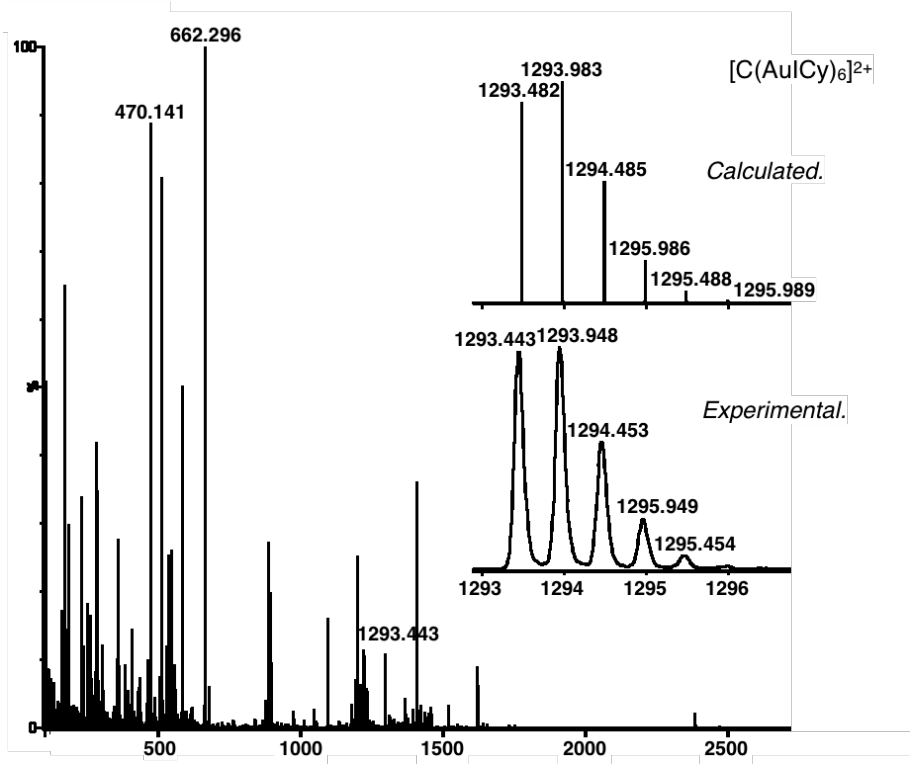

Figure 2-4-2. An ESI-TOF MS spectrum of $[C(AuICy)_6]^{2+}$ (positive, acetonitrile, Capillary: 3000 V; Sample cone: 30 V).

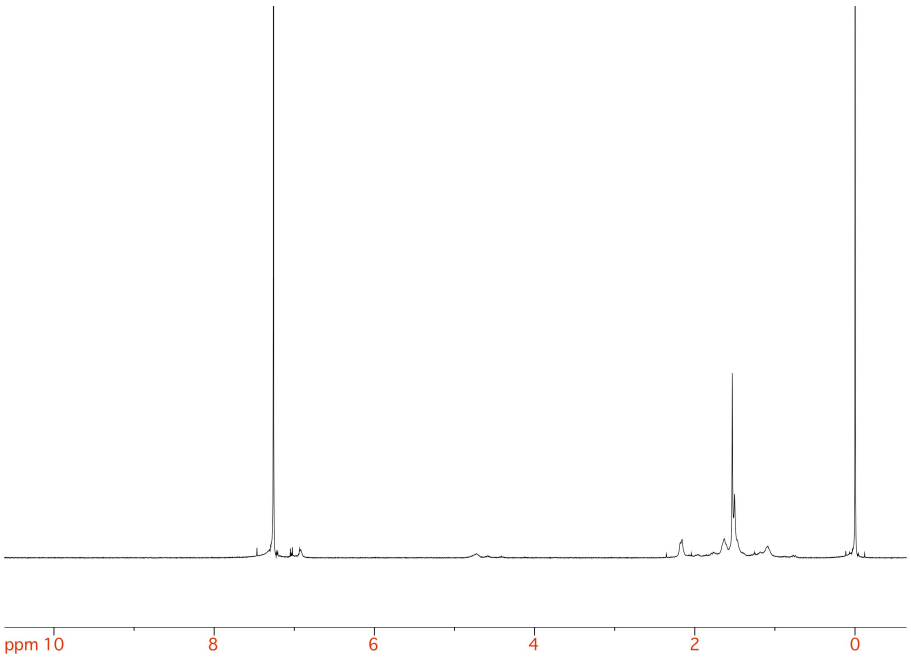

Figure 2-4-3. A ^1H NMR spectrum of the reaction between $[O(AuICy)_3]\cdot(BF_4)$ and $TMSCHN_2$ (500 MHz, 300 K, CD_3CN).

2.5 Conclusions

In this chapter, I have reported the synthesis of an *N*-heterocyclic carbene ligand-supported, carbon-centered Au^I cluster $[C(AuI\mathit{i}Pr)_6]\cdot(BF_4)_2$, and characterized its structure and properties by ^1H and ^{13}C NMR, ESI-TOF MS, and XRD analyses. This compound is chemically stable and easily handled under ambient conditions.

To clarify the ligand effects on the CAu^I_6 core structure, the crystal structure and photoluminescence properties of I*i*Pr-supported $[C(AuI\mathit{i}Pr)_6]\cdot(BF_4)_2$ were further investigated and compared in detail with the PPh_3-supported counterparts $[C(AuPPh_3)_6]\cdot(CH_3OBF_3)_2$ and $[C(AuPPh_3)_6]\cdot(BF_4)_2$ reported by Schmidbaur *et al*. Even these clusters have common features, the $[C(AuI\mathit{i}Pr)_6]\cdot(BF_4)_2$ complex prepared in this study showed a unique antiprism structure with D_{3h} symmetry, while PPh_3-supported carbon-centered Au^I clusters have lower or almost no crystallographic symmetry. In addition, this complex showed luminescence in the solid state at a longer wavelength compared to that of a PPh_3-supported counterpart, which may come from the stronger σ-coordination ability of NHC ligands. All of these clusters exhibited almost no emission in the solution state at room temperature. Construction of carbon-centered Au^I clusters supported by two other NHC ligands: 1,3-bis(2,4,6-trimethylphenyl)imidazol-2-ylidene (IMes) and 1,3-bis(cyclohexyl)imidazol-2-ylidene (ICy) were also illustrated in this chapter. Based on these results it was clearly confirmed that the supporting ligand significantly affects the steric and electronic structures of the resultant carbon-centered Au^I clusters.

NHC ligands have great advantages in terms of easy and therefore diverse chemical modification of their steric and electronic structures. The results described in this chapter would widen the basis for further studies and applications for homo- and heterometallic carbon-centered coinage metal clusters.

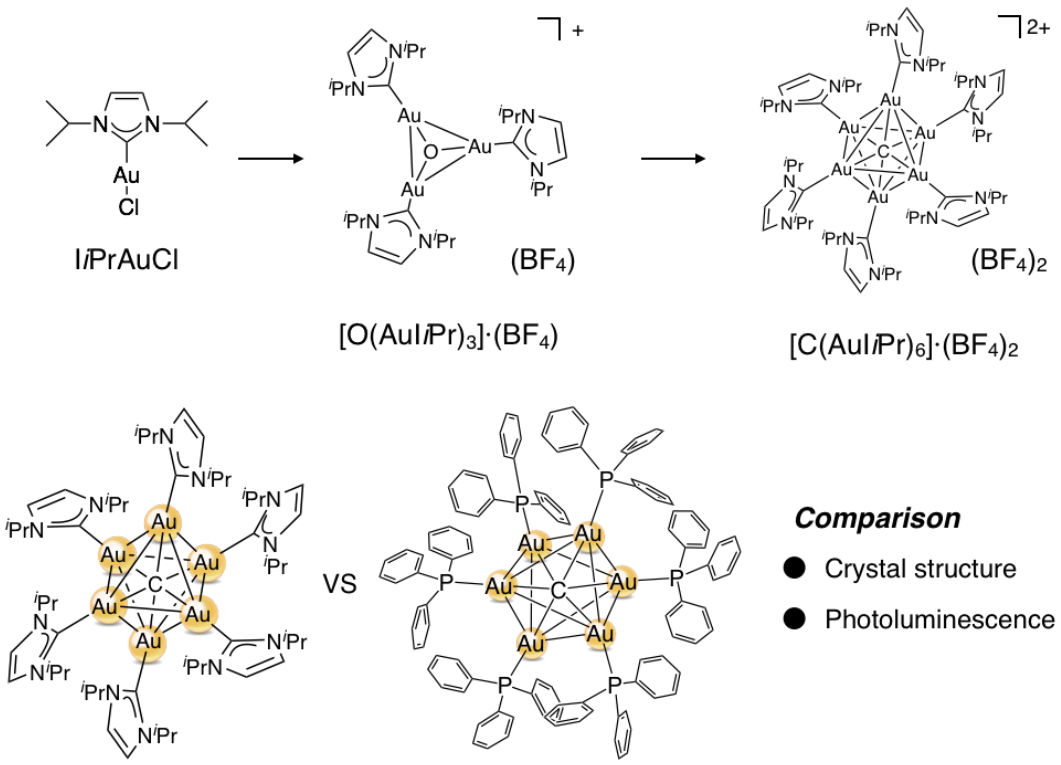

Figure 2-5-1. Synthesis of I*i*Pr-supported carbon-centered Au^{I} clusters and their comparison with PPh_3-supported counterparts.

2.6 Experimental Section

Materials and methods

Unless otherwise noted, solvents and reagents were purchased from TCI Co., Ltd., Fujifilm WAKO Pure Chemical Co., Kanto Chemical Co., and Sigma-Aldrich Co., and used without further purification. Chloro(tetrahydrothiophene)gold(I), $ClAu(SC_4H_8)$, was synthesized according to the literature.[11]

^1H, ^{13}C NMR spectra were recorded on a Bruker AVANCE III spectrometer. All ^1H NMR spectra are reported in δ units, parts per million (ppm) downfield from tetramethylsilane (TMS) as the internal standard or relative to the central line of the quintet for CD_2HCN at 1.94 ppm. The following abbreviations are used: s = singlet, d = doublet, t = triplet, q = quadruplet, sept = septet, m = multiplet, br = broad). All ^{13}C NMR spectra were reported in ppm relative to the central line of the triplet for $CDCl_3$ at 77.16 ppm, the single for CD_3CN at 118.26 ppm.

X-ray crystallographic analyses were performed using a Rigaku XtaLAB P200 imaging plate diffractometer with CuKα radiation, and obtained data were calculated using the Crystal Structure crystallographic software package except for refinement, which was performed using SHELXL Version 2013/4.[12] All hydrogen atoms were placed geometrically and refined using a riding model. Crystallographic data can be obtained free of charge from the Cambridge Crystallographic Data Centre (http://www.ccdc.cam.ac.uk/data_request/cif).

ESI-TOF MS data were recorded on a Micromass LCT Premier XE mass spectrometer. Unless otherwise noted, experimental conditions were as follows (Ion mode, positive; Capillary voltage, 3000 V; Sample cone voltage, 30 V; Desolvation temperature, 150 °C; Source temperature, 80 °C).

Melting points were measured by Yanaco Micro Melting Point Apparatus MP-500D.

UV-vis spectra were recorded on a JASCO V-770 UV-vis spectrophotometer. Emission and excitation spectra were recorded on a Fluorolog-NIR-HORIBA fluorescence spectrophotometer. Elemental analysis was conducted in the Microanalytical Laboratory, Department Chemistry, School of Science, the University of Tokyo.

Synthesis of hexakis-gold(I) methanium salt $[C(AuI\mathit{i}Pr)_6]\cdot(BF_4)_2$

Compound $[C(AuI\mathit{i}Pr)_6]\cdot(BF_4)_2$ was synthesized according to Scheme 2-6-1. Synthesis of Chloro(tetrahydrothiophene)gold(I) $ClAu(SC_4H_8)$ was reported previously.[11]

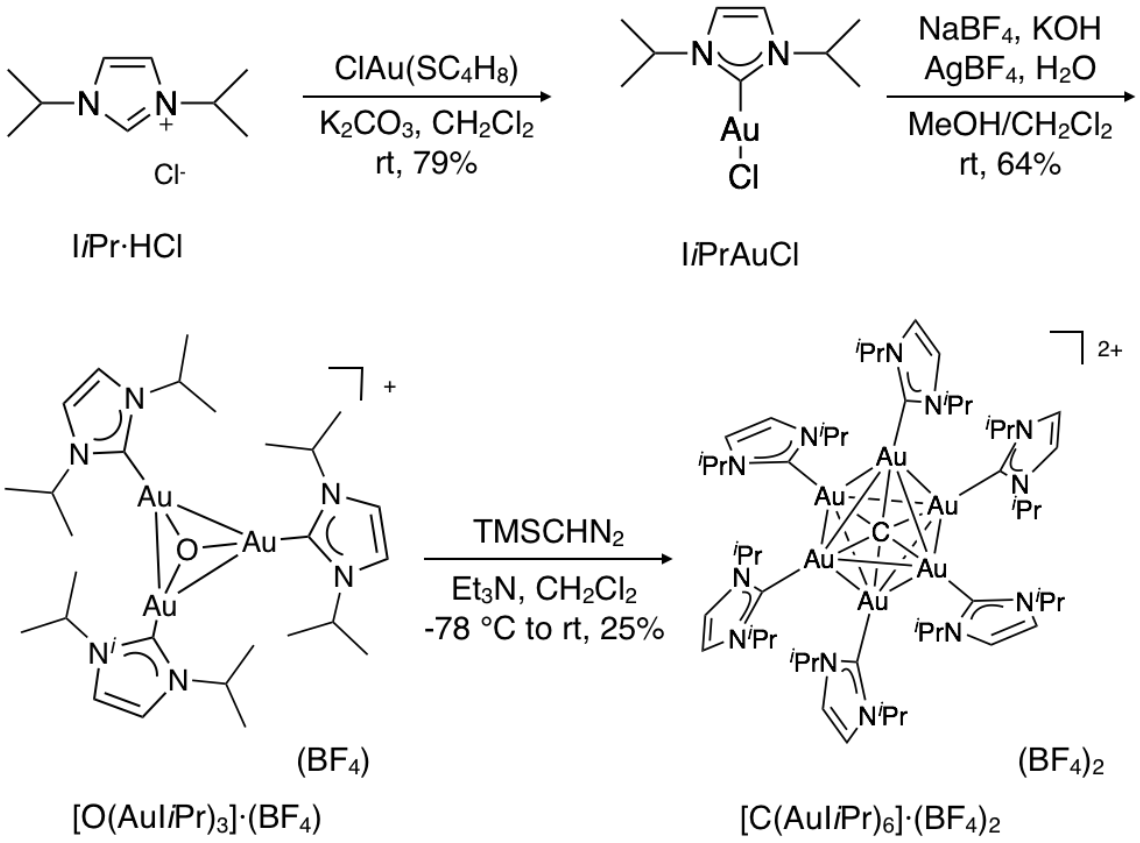

Scheme 2-6-1. Synthesis of compound $[C(AuI\mathit{i}Pr)_6]\cdot(BF_4)_2$.

Synthesis of chloro[1,3-bis(isopropyl)imidazol-2-ylidene]gold(I) I*i*PrAuCl

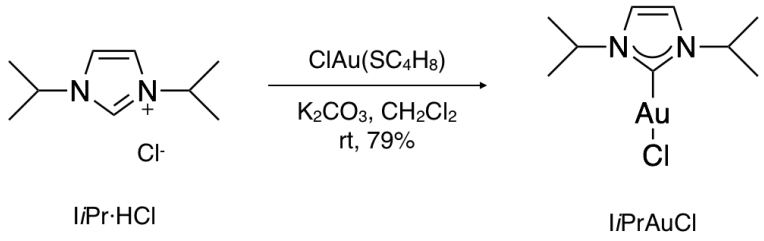

I*i*Pr·HCl　　I*i*PrAuCl

A mixture of I*i*Pr·HCl (0.190 g, 1.01 mmol) and $ClAuSC_4H_8$ (0.320 g, 1.00 mmol) in CH_2Cl_2 (43 mL) was stirred for 15 min and then K_2CO_3 (2.76 g, 20.0 mmol) was added. After 8 h, the mixture was filtered and the solvent was removed in vacuo. The product was purified by passing through a short path of silica (CH_2Cl_2 3 mL × 3). I*i*PrAuCl was obtained as a colorless solid (0.305 g, 0.794 mmol, 79%).

^{1}H NMR (500 MHz, 300 K, $CDCl_3$): δ 6.98 (s, 2 H), 5.05 (sept, J = 6.8 Hz, 2 H), 1.47 (d, J = 6.8 Hz, 12 H).
^{13}C NMR (126 MHz, 300 K, $CDCl_3$): δ 168.5, 116.7, 53.7, 23.4.

Synthesis of tris[(1,3-bis(isopropyl)imidazol-2-ylidene)gold(I)]oxonium tetrafluoroborate $[O(AuI\mathit{i}Pr)_3]\cdot(BF_4)$

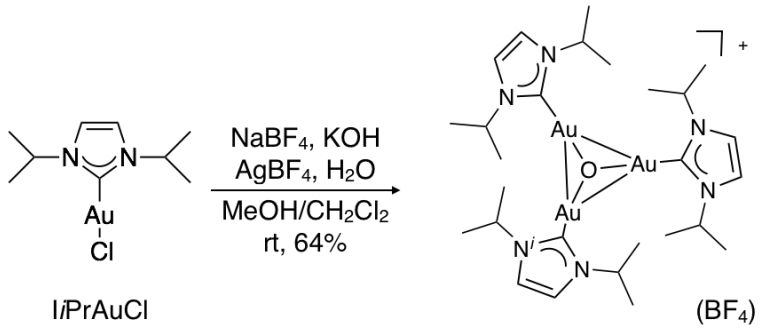

I*i*PrAuCl　　$[O(AuI\mathit{i}Pr)_3]\cdot(BF_4)$

A solution of I*i*PrAuCl (192 mg, 0.500 mmol) in CH_2Cl_2 (10 mL) was added to a solution of KOH (50.0 mg, 0.909 mmol) and $NaBF_4$ (252 mg, 2.29 mmol) in MeOH (50 mL). After addition of $AgBF_4$ (92.0 mg, 0.474 mmol) in MeOH (2 mL), AgCl was immediately precipitated, and then 3 mL of H_2O was added to the mixture. After

stirring at room temperature for 1 h, the solvents were evaporated under reduced pressure. The crude product was extracted by CH_2Cl_2, and reprecipitated by CH_2Cl_2/diethyl ether to afford $[O(AuI\textit{i}Pr)_3]\cdot(BF_4)$ as a colorless solid (120 mg, 0.104 mmol, 62%).

^{1}H NMR (500 MHz, 300 K, $CDCl_3$): δ 7.06 (s, 6 H), 5.05 (sept, J = 6.8 Hz, 6 H), 1.50 (d, J = 6.8 Hz, 36 H).
^{13}C NMR (126 MHz, 300 K, $CDCl_3$): δ 159.9, 117.1, 53.5, 23.3.
HRMS (CH_3CN, positive): $[O(AuI\textit{i}Pr)_3]^+$ ($C_{27}H_{48}Au_3N_6O$) *m/z* 1063.2891 (required, 1063.2886).

Synthesis of I*i*Pr-supported hexagold(I)methanium salt, $[C(AuI\textit{i}Pr)_6]\cdot(BF_4)_2$

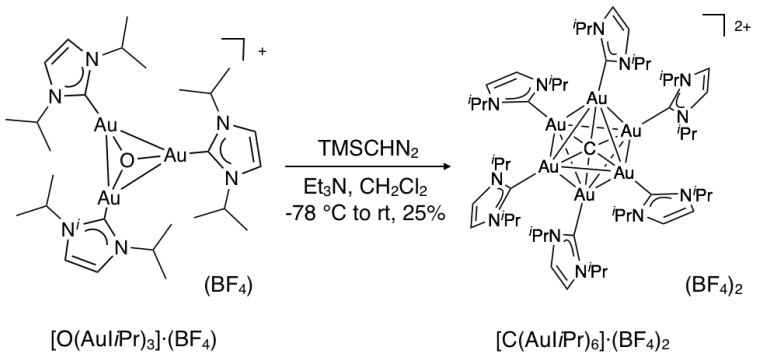

A solution of (trimethysilyl)diazomethane in *n*-hexane (52 μL, 2.0 M, 0.100 mmol) was added to a solution of $[O(AuI\textit{i}Pr)_3]\cdot(BF_4)$ (120 mg, 0.104 mmol) in dry CH_2Cl_2 at -78 °C in the presence of triethylamine (15 μL, 0.100 mmol), and the solution was allowed to warm to room temperature and stirred for additional 1 h. After reprecipitation by CH_3CN/diethyl ether three times, $[C(AuI\textit{i}Pr)_6]\cdot(BF_4)_2$ was obtained as a dark-brown solid (31.0 mg, 0.0136 mmol, 25%).

^{1}H NMR (500 MHz, 300 K, CD_3CN): δ 7.09 (s, 12 H), 5.11 (sept, J = 6.8 Hz, 12 H), 1.34 (d, J = 6.8 Hz, 72 H).
^{13}C NMR (126 MHz; 300 K, CD_3CN): δ 182.3, 117.1, 53.3, 23.4.
Melting point: 258–260 °C (decomposition).
HRMS (CH_3OH, positive): $[C(AuI\textit{i}Pr)_6]^{2+}$ ($C_{55}H_{96}Au_6N_{12}$) *m/z* 1053.2937 (required,

1053.2932).

Anal. Calcd. for $C_{55}H_{96}Au_6B_2F_8N_{12}\cdot 3H_2O$ (2334.88): C, 28.29; H, 4.40; N, 7.20. Found: C, 28.21; H, 4.18; N, 7.00.

Synthesis of hexakis-gold(I) methanium salt $[C(AuICy)_6]\cdot(BF_4)_2$

Compound $[C(AuICy)_6]\cdot(BF_4)_2$ was synthesized according to Scheme 2-6-2. Synthesis of Chloro(tetrahydrothiophene)gold(I) $ClAu(SC_4H_8)$ was reported previously.[11]

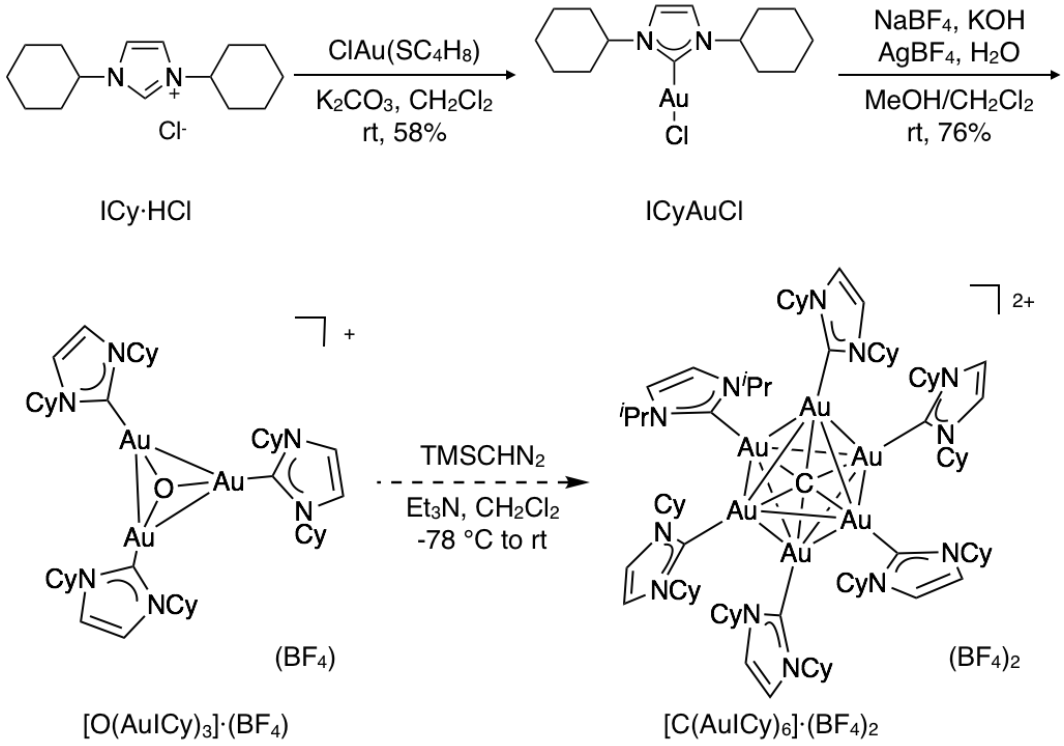

Scheme 2-6-2. Synthesis of compound $[C(AuICy)_6]\cdot(BF_4)_2$.

Synthesis of chloro[1,3-bis(cyclohexyl)imidazol-2-ylidene]gold(I) ICyAuCl

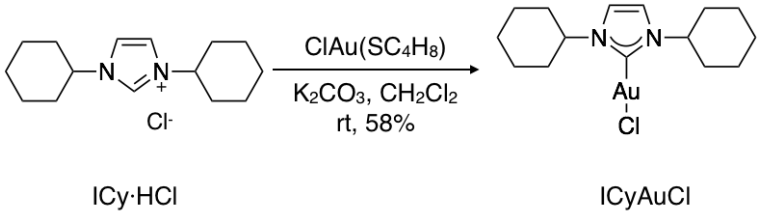

ICy·HCl ICyAuCl

A mixture of 1,3-bis(cyclohexyl)imidazolium chloride (0.268 g, 1.00 mmol) and $AuCl(SC_4H_8)$ (0.325 g, 1.02 mmol) in CH_2Cl_2 (15 mL) was stirred for 15 min, and then K_2CO_3 (2.73 g, 19.8 mmol) was added. After 4 h, the inorganic salts were removed and then the solvent was evaporated to afford ICyAuCl as a colorless solid (0.273 g, 0.588 mmol, 59%). This crude material was used for the next step without further purification.

^{1}H NMR (500 MHz, 300 K, $CDCl_3$): δ 6.95 (s, 2 H), 4.60 (tt, *J* = 11.8, 3.9 Hz, 2 H), 2.13–2.06 (m, 4 H), 1.91–1.84 (m, 4 H), 1.80–1.73 (m, 2 H), 1.57 (qd, *J* = 12.7, 3.4 Hz, 4 H), 1.48 (qt, *J* = 13.1, 3.2 Hz, 4 H), 1.20 (qt, *J* = 12.9, 3.7 Hz, 2 H).

Synthesis of tris[(1,3-bis(cyclohexyl)imidazol-2-ylidene)gold(I)]oxonium tetrafluoroborate $[O(AuICy)_3]\cdot(BF_4)$

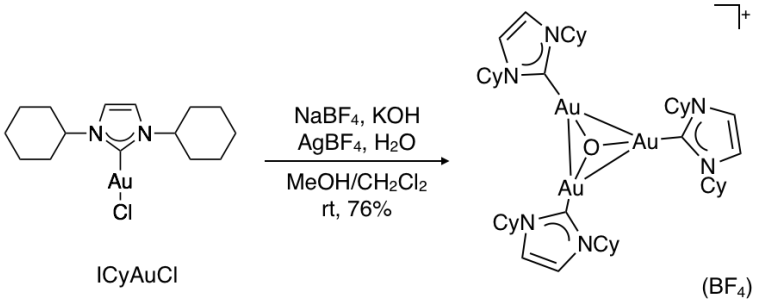

ICyAuCl $[O(AuICy)_3]\cdot(BF_4)$

A solution of ICyAuCl (233mg, 0.502 mmol) in CH_2Cl_2 (10 mL) was added to a solution of KOH (50.0 mg, 0.893 mmol) and $NaBF_4$ (252 mg, 2.29 mmol) in 50 mL MeOH. After addition of $AgBF_4$ (97.0 mg, 0.500 mmol) in 2 mL MeOH to the solution, a colorless precipitate of AgCl was observed immediately, and then 3 mL of H_2O was

added. After stirring at room temperature for 1 h, AgCl was removed and the solvents were evaporated under reduced pressure. The crude product was extracted by CH_2Cl_2 and reprecipiated by adding CH_2Cl_2/diethyl ether to afford $[O(AuICy)_3]\cdot(BF_4)$ as a pale-brown solid (177 mg, 0.127 mmol, 76%)

^{1}H NMR (500 MHz, 300 K, $CDCl_3$): δ 7.05 (s, 6 H), 4.64–4.58 (m, 6 H), 2.12–2.06 (m, 12 H), 1.90–1.80 (m, 12 H), 1.72–1.61 (m, 18 H), 1.36–1.20 (m, 18 H).
^{13}C NMR (126 MHz, 300 K, $CDCl_3$): δ 160.2, 117.5, 60.9, 33.9, 25.5, 25.0.
ESI-TOF MS (CH_3CN, positive): found: m/z = 1303.48, calculated for $C_{45}H_{72}Au_3N_6O^+$ ($[O(AuICy)_3]^+$): m/z = 1303.48.

Synthesis of hexakis[(1,3-bis(cyclohexyl)imidazol-2-ylidene)gold(I)]methanium bis(tetrafluoroborate) $[C(AuICy)_6]\cdot(BF_4)_2$

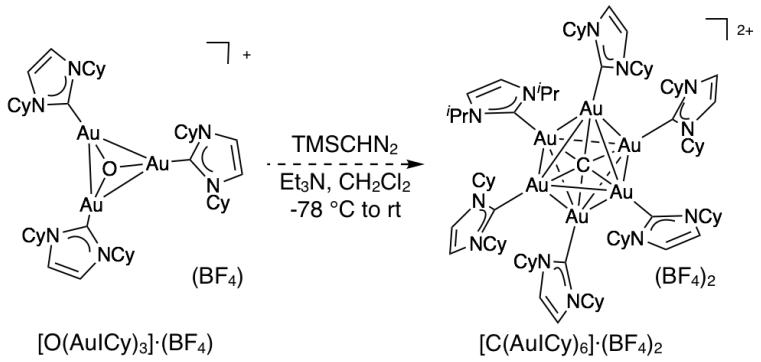

Triethylamine (15 μL, 0.101 mmol) and a 2.0 M *n*-hexane solution of trimethysilyldiazomethane (52 μL, 0.101 mmol) were added to a solution of $[O(AuICy)_3]\cdot(BF_4)$ (144 mg, 0.104 mmol) in dry CH_2Cl_2 (2 mL) at -78 °C. The resulting mixture was warmed up to room temperature gradually and stirred at room temperature for 3 h. This reaction was monitored by ^{1}H NMR spectrum as well as ESI-TOF MS measurements

Synthesis of IMes-supported carbon-centered Au^I cluster

IMes supported carbon-centered Au^I clusters were synthesized according to Scheme 2-6-3. Synthesis of chloro(tetrahydrothiophene)gold(I) $ClAu(SC_4H_8)$ was reported previously.[11]

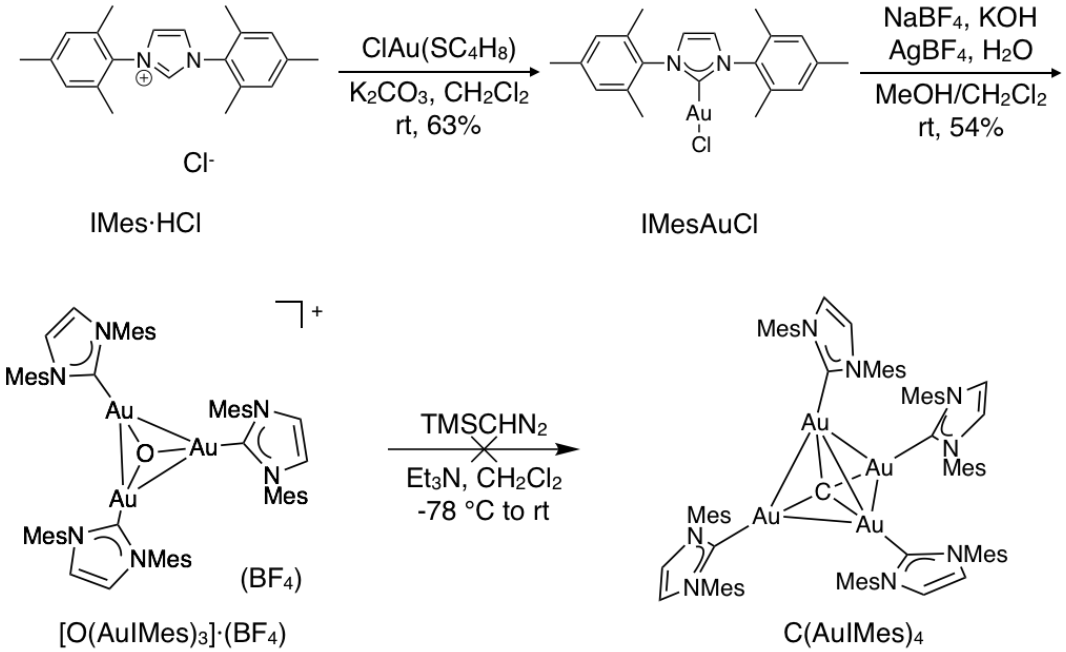

Scheme 2-6-3. Synthesis of compound $C(AuIMes)_4$.

Synthesis of chloro[1,3-bis(2,4,6-trimethylphenyl)imidazol-2-ylidene]gold(I) (IMesAuCl)

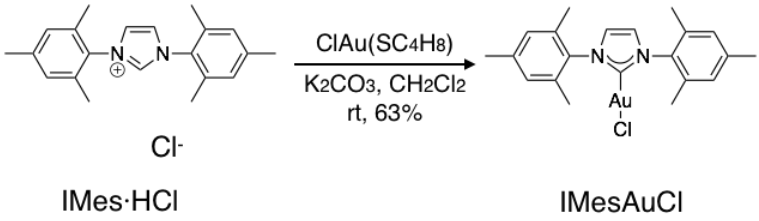

A mixture of IMes·HCl (0.118 g, 0.347 mmol) and $ClAu(SC_4H_8)$ (0.112 g, 0.350 mmol) in CH_2Cl_2 (15 mL) was stirred for 15 min, and then K_2CO_3 (0.967 g, 7.01 mmol) was added. After 1.5 h, the mixture was filtered through Celite, then the solvent was evaporated and crude product was obtained as a pale-gold solid. The crude product was repreciptated with CH_2Cl_2/Et_2O. IMesAuCl was obtained as a colorless solid (0.118 g, 0.220 mmol, 63%).

^{1}H NMR (500 MHz, 300 K, $CDCl_3$): δ 7.09 (s, 2 H), 6.99 (s, 4 H), 2.34 (s, 6 H), 2.10 (s, 12 H).

Synthesis of tris[(1,3-bis(2,4,6-trimethylphenyl)imidazol-2-ylidene)gold(I)]oxonium tetrafluoroborate $[O(AuIMes)_3]\cdot(BF_4)$

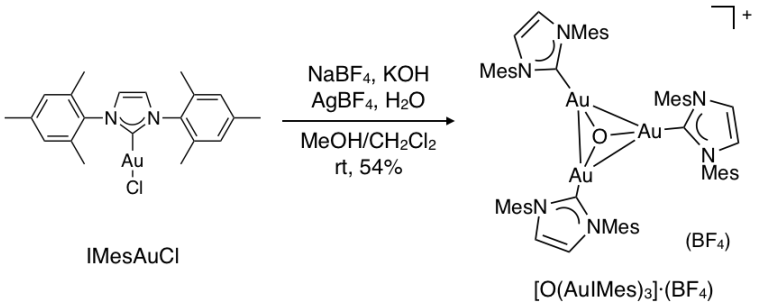

A solution of IMesAuCl (0.263 g, 0.50 mmol) in CH_2Cl_2 (10 mL) was added to a solution of KOH (50.0 mg, 0.893 mmol) and $NaBF_4$ (0.267 g, 2.43 mmol) in 40 mL MeOH. $AgBF_4$ (97.0 mg, 0.500 mmol) in 2.0 mL MeOH was added; a colorless precipitate of AgCl was observed immediately and followed by the addition of 3.0 mL

of water. After stirring at room temperature for 1 h, the solvents were removed under reduced pressure, and the residue was extracted by CH_2Cl_2. After removal of the solvent, the crude product was further purified by reprecipitation with CH_2Cl_2/Et_2O. $[O(AuIMes)_3]\cdot(BF_4)$ was obtained as a colorless solid (146 mg, 0.0909 mmol, 55%).

^{1}H NMR (500 MHz, 300 K, $CDCl_3$): δ 7.02 (s, 6 H), 6.91 (s, 12 H), 2.34 (s, 18 H), 1.95 (s, 36 H).
^{13}C NMR (126 MHz, 300 K, $CDCl_3$): δ 164.8, 139.0, 134.8, 134.5, 129.2, 122.3, 21.2, 17.7.
ESI-TOF MS: found: *m*/*z* = 1519.48, calculated for $C_{63}H_{72}Au_3N_6O^+$ $[O(AuIMes)_3]^+$: *m*/*z* = 1519.48.

The reaction between $[O(AuIMes)_3]\cdot(BF_4)$ with $TMSCHN_2$

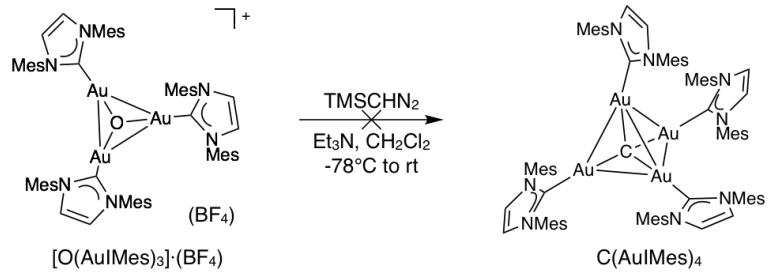

$[O(AuIMes)_3]\cdot(BF_4)$ $C(AuIMes)_4$

Triethylamine (15 μL, 0.100 mmol) and a 2.0 M hexane solution of trimethysilyldiazomethane (52 μL, 0.100 mmol) were added to a solution of $[O(AuIMes)_3]\cdot(BF_4)$ (144 mg, 0.0896 mmol) in dry CH_2Cl_2 (2 mL) at -78 °C. The resulting mixture was warmed up to room temperature gradually and stirred at room temperature for 3 h. This reaction was monitored by ^{1}H NMR spectrum as well as ESI-TOF MS measurements.

Single-crystal X-ray analysis of $[C(AuI\mathit{i}Pr)_6]\cdot(BF_4)_2$

Crystals suitable for X-ray analysis were obtained by slow vapor evaporation of a saturated solution of $[C(AuI\mathit{i}Pr)_6]\cdot(BF_4)_2$ in CH_2Cl_2/*n*-hexane at room temperature.

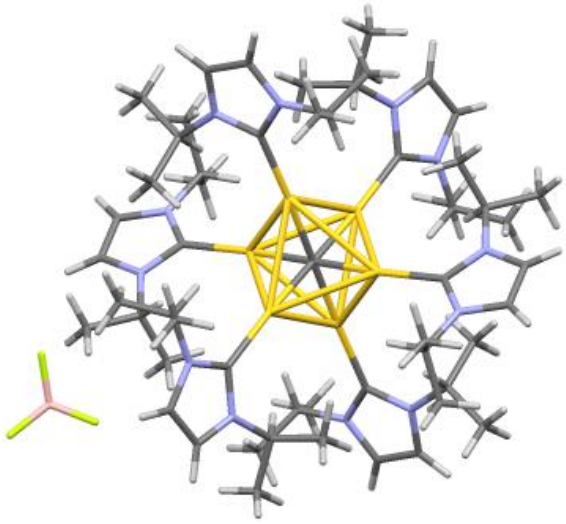

Figure 2-6-1. Crystal Structure of $[C(AuI\mathit{i}Pr)_6]\cdot(BF_4)_2$ with stick model. Color code; Au gold, C gray, N blue, B pink, F green, H white. Crystal data for $[C(AuI\mathit{i}Pr)_6]\cdot(BF_4)_2$: $C_{55}H_{96}Au_6B_2F_8N_{12}$, Fw = 2280.85, yellow, block, 0.028 × 0.063 × 0.188 mm^3, trigonal, space group *P*-3 (#147), a = 13.87654 (9) Å, c = 10.17974(8) Å, V = 1697.58(2) $Å^3$, Z = 1, ρ_{calc} = 2.146 g/cm^3, T = 93 K, λ(CuKα) = 1.54187 Å, $2\theta_{max}$ = 136.3°, 2080/10144 reflections collected/unique (R_{int} = 0.0389), R_1 = 0.0244 ($I > 2\sigma(I)$), wR_2 = 0.0603 (for all data), GOF = 1.187, largest diff. peak and hole 1.05/-1.43 $eÅ^{-3}$. CCDC Deposit number 1838792.

Tris[(1,3-bis(isopropyl)imidazol-2-ylidene)gold(I)]oxonium tetrafluoroborate $[O(AuI\mathit{i}Pr)_3]\cdot(BF_4)$

$C_{27}H_{48}Au_3BF_4N_6O\cdot CH_2Cl_2$, *Mr* = 1233.34, triclinic, *P*-1 (#2), *a* = 14.3525(11) Å, *b* = 14.4241(10) Å, *c* = 20.7034(11) Å, α = 82.174(2)°, β = 80.679(2)°, γ = 59.762(2)°, *V* = 3653.9(4) Å^3, *Z* = 4, *Dcalc* = 2.242 g/cm^3, MoKα, λ = 0.71075 Å, F_{000} = 2312, *temp* = -180.0 °C, final *R* = 0.0839 for 16433 unique reflections.

Tris[(1,3-bis(cyclohexyl)imidazol-2-ylidene)gold(I)]oxonium tetrafluoroborate $[O(AuICy)_3]\cdot(BF_4)$

$C_{45}H_{72}Au_3BF_4N_6O\cdot CH_2Cl_2$, *Mr* = 1475.74, triclinic, *P*-1 (#2), *a* = 13.9309(7) Å, *b* = 14.2648(7) Å, *c* = 14.5243(7) Å, α = 101.0830(14)°, β = 98.1861(15)°, γ = 106.4469(15)°, *V* = 2656.5(2) Å^3, *Z* = 2, *Dcalc* = 1.845 g/cm^3, MoKα, λ = 0.71075 Å, F_{000} = 1424.00, *temp* = -180.0 °C, final *R* = 0.0353 for 11911 unique reflections.

Tris[(1,3-bis(mesityl)imidazol-2-ylidene)gold(I)]oxonium tetrafluoroborate $[O(AuIMes)_3]\cdot(BF_4)$

$C_{63}H_{72}Au_3BF_4N_6O$ $0.5CH_2Cl_2$, Mr = 1649.47, triclinic, *P*-1 (#2), *a* = 16.6938(7) Å, *b* = 20.3330(8) Å, *c* = 24.0981(9) Å, α = 113.7442(11)°, β = 90.3484(13)°, γ = 110.8476(12)°, *V* = 6887.1(5) Å^3, *Z* = 4, *Dcalc* = 1.591 g/cm^3, MoKα, λ = 0.71075 Å, F_{000} = 3196, *temp* = -180.0 °C, final *R* = 0.0452 for 30385 unique reflections

UV-vis absorption and emission spectra of $[C(AuI\mathit{i}Pr)_6]\cdot(BF_4)_2$

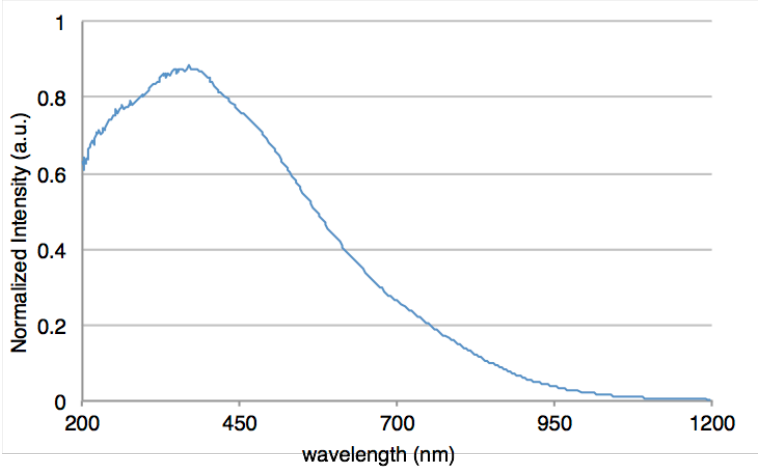

Figure 2-6-2. UV-vis-NIR absorption spectrum of $[C(AuI\mathit{i}Pr)_6]\cdot(BF_4)_2$ in the solid state at 293 K.

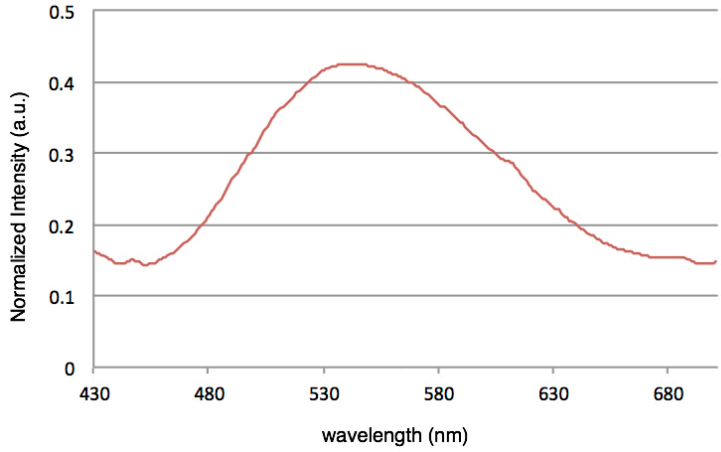

Figure 2-6-3. Emission spectrum of $[C(AuI\mathit{i}Pr)_6]\cdot(BF_4)_2$ in the solid state (λ_{ex} 370 nm) at 293 K.

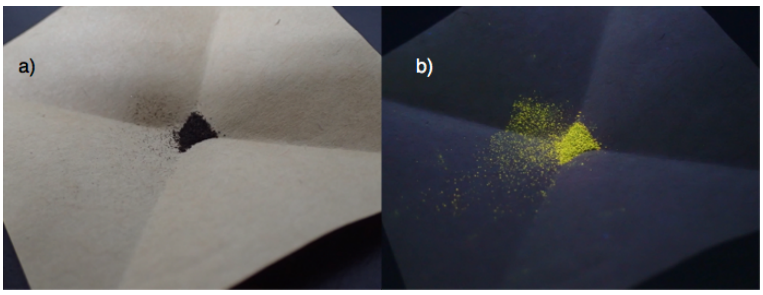

Figure 2-6-4. Pictures of $[C(AuI\mathit{i}Pr)_6]\cdot(BF_4)_2$ in the solid state at room temperature: a) under natural light and b) under photo-irradiation by UV lamp (365 nm).

2.7 References

1. a) F. Scherbaum, A. Grohmann, B. Huber, C. Krüger, H. Schmidbaur, *Angew. Chem. Int. Ed. Engl.*, **1988**, *27*, 1544–1546; b) F. Scherbaum, A. Grohmann, G. Müller, H. Schmidbaur, *Angew. Chem. Int. Ed. Engl.*, **1989**, *28*, 463–465; c) H. Schmidbaur, O. Steigelmann, *Z. Naturforsch. B*, **1992**, *47*, 1721–1724; d) F. P. Gabbaï, A. Schier, J. Riede, H. Schmidbaur, *Chem. Ber.*, **1997**, *130*, 111–113.

2. J.-H. Jia, Q. -M. Wang, *J. Am. Chem. Soc.*, **2009**, *131*, 16634–16635.

3. Z. Lei, X. -L. Pei, Z. -G. Jiang, Q. -M. Wang, *Angew. Chem. Int. Ed.*, **2014**, *53*, 12771–12775.

4. D. S. Matteson, J. R. Thomas, *J. Organomet. Chem.*, **1970**, *24*, 263–271.

5. R. Visbal, A. Laguna, M. C. Gimeno, *Chem. Commun.,* **2013**, *49*, 5642–5644.

6. A. N. Nesmeyanov, E. G. Perevalova, Y. T. Struchkov, M. Y. Antipin, K. I. Grandberg, V. P. Dyadhenko, *J. Organomet. Chem.*, **1980**, *201*, 343–349.

7. Y. Yang, V. Ramamoorthy, P. R. Sharp, *Inorg. Chem.*, **1993**, *32,* 1946–1950.

8. H. Schmidbaur, B. Brachthauser, O. Steigelmann, *Angew. Chem. Int. Ed. Engl.*, **1991**, *30*, 1400–1490.

9. H. Schmidbaur, *Chem. Soc. Rev.*, **1995**, *24*, 391–400.

10. H. G. Raubenheimer, S.Cronje, *Chem. Soc. Rev.*, **2008**, *37*, 1998−2011.

11. S. H. Jung, J. Jeon, H. Kim, J. Jaworski, J. H. Jung, *J. Am. Chem. Soc.*, **2014**, *136*, 6446–6452.

12. G.M. Sheldrick, *Acta Cryst.,* **2008**, *A64*, 112–122.

3. Dinuclear Au^{I}-based double helix with conformationally flexible bis-NHC ligands

本章については、5年以内に雑誌等で刊行予定のため、非公開。

4. Conclusions

In this study, I have focused on the construction of multinuclear Au^I complexes with *N*-heterocyclic carbene (NHC) ligands. Specifically, a carbon-centered CAu^I_6 cluster and a macrocyclic dinuclear Au^I compound based on bis-NHC ligands have been developed for Au-based multinuclear complexes with structure-specific properties. Here, as part of my continuing study of master course, I have constructed a carbon-centered CAu^I_6 cluster with an antiprism structure. Ligand effects on structure, photochemical and redox properties are further examined. Furthermore, a helical macrocyclic dinuclear Au^I compound based on a bis-NHC ligand were constructed, and the redox behaviors and luminescent properties have been clarified.

In **Chapter 2,** I have reported the synthesis of an *N*-heterocyclic carbene ligand-supported, carbon-centered Au^I cluster $[C(AuI\mathit{i}Pr)_6]\cdot(BF_4)_2$, and characterized its structure and properties by ^1H and ^{13}C NMR, ESI-MS, and XRD analyses. This compound is chemically stable and easily handled under ambient conditions. To find out the ligand effects on the structure-specific properties, the crystal structure and photoluminescence properties of I*i*Pr-supported $[C(AuI\mathit{i}Pr)_6]\cdot(BF_4)_2$ are in comparison with the PPh_3-supported counterparts reported by Schmidbaur *et al.* in considerable detal. Construction of carbon-centered Au^I clusters supported by two other NHC ligands: 1,3-bis(2,4,6-trimethylphenyl)imidazol-2-ylidene (IMes) and 1,3-bis(cyclohexyl)imidazol-2-ylidene (ICy) were also illustrated in this chapter. All the results indicate that the supporting ligand could significantly affect the resultant carbon-centered Au^I clusters.

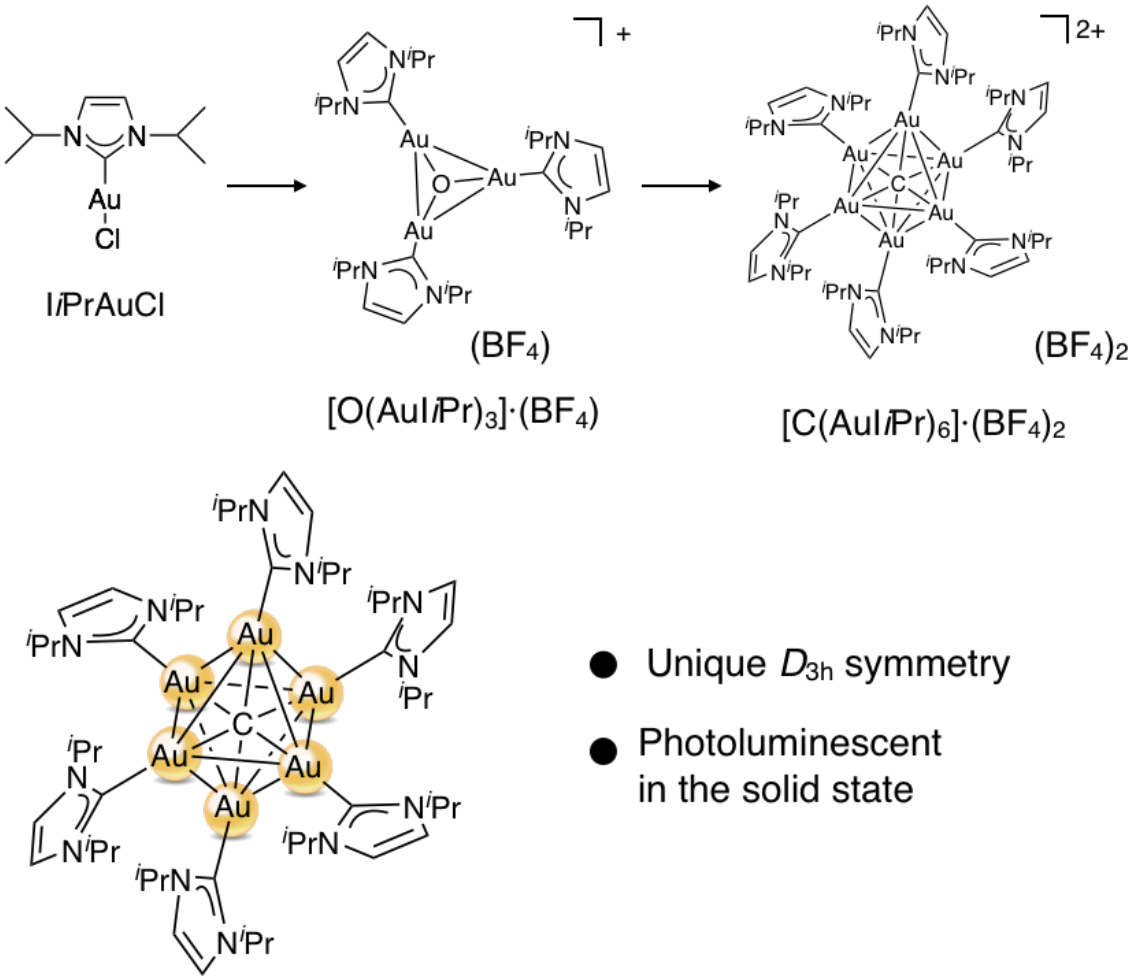

Figure 4-1. Summary of **Chapter 2**.

In **Chapter 3**, I have developed a bis-NHC ligand **L** with a pyridine-centered heterocycle-coupled spacer and constructed an Au^I-mediated macrocycle bearing **L**, which shows a unique helical structure. The precursor of ligand **L**, a bis-imidazolium salt $H_2\mathbf{L}\cdot(PF_6)_2$, was synthesized from 2-acetylfuran in 6 steps. Complexation of $H_2\mathbf{L}\cdot(PF_6)_2$ with equimolar amount of $ClAu(SC_4H_8)$ generates a macrocyclic dinuclear Au^I complex, $[\mathbf{L}_2Au^I_2](PF_6)_2$, which is air-, light- and moisture-stable under ambient conditions. $[\mathbf{L}_2Au^I_2](PF_6)_2$ exhibits a high symmetrical structure in solution, suggesting the free rotation around the single bond between heteroaromatic rings. On the other hand, single crystal X-ray analysis of $[\mathbf{L}_2Au^I_2](PF_6)_2$ established a helical structure. Adding chiral counter anions to the solution of $[\mathbf{L}_2Au^I_2](PF_6)_2$ could not induce chiral discrimination nor asymmetric induction. Both in solution and in the solid state, bis-imidazolium salts, $H_2\mathbf{L}\cdot(PF_6)_2$ and $[\mathbf{L}_2Au^I_2]\cdot(PF_6)_2$, show similar photoluminescence

behaviors. Introduction of other metal ions into the central cavity of macrocyclic $[\mathbf{L}_2Au^{I}_2]\cdot(PF_6)_2$ failed due to its narrow helical structure. On the other hand, an unexpected halogen-based oxidation reaction of Au^{I} centers to Au^{III} centers was observed. Further study will focus on enantio-diffentiation, as well as redox-inducing helicity switching and metal array-induced helicity switching.

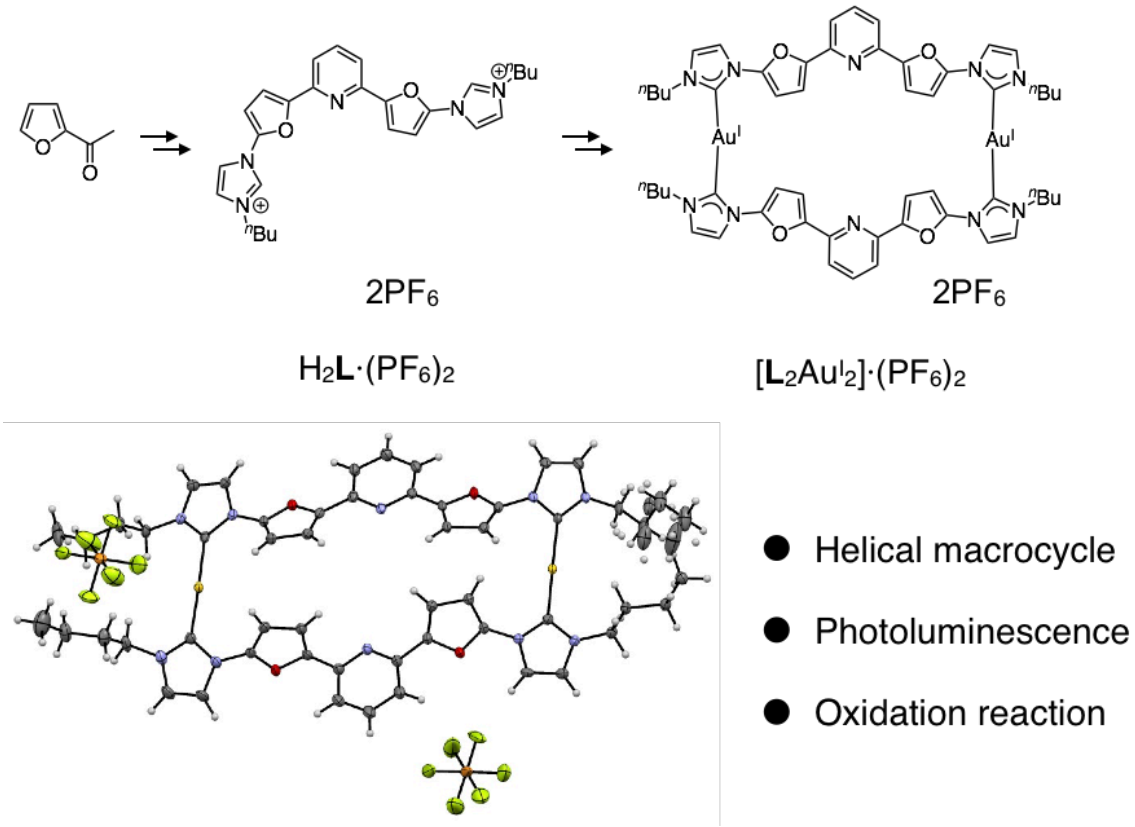

Figure 4-2. Summary of **Chapter 3**.

Further study concerning the Au^{I}-based multinuclear compounds will focus on their photochemical and electronic properties and multi-electron-based catalytic activity.

A list of publications

[1]. “A Carbon-Centered Hexagold(I) Cluster Supported by N-Heterocyclic Carbene Ligands” Hitoshi Ube, Qian Zhang, and Mitsuhiko Shionoya, *Organometallics*, **2018**, *37*(13), 2007–2009.

Acknowledgement

This research was promoted under supervision of Professor Dr. Mitsuhiko Shionoya (The University of Tokyo). He has always given me generous guidance, reassuring encouragement and inspired ideas. I cannot express my appreciation enough for his fruitful discussion and extraordinary care for my life as a researcher for five years. I would like to take this opportunity to express my utmost gratitude to him.

I deeply appreciated Assistant Professor Dr. Hitoshi Ube (The university of Tokyo) for his patient, kind teaching and critical suggestion about my research. His innovative, creative, and progressive ideas have always expanded my view of science.

I appreciate Associate Professor Dr. Shohei Tashiro (The university of Tokyo) for his kind teaching and fruitful and inspiring discussion and suggestion about chemistry.

I am thankful to Assistant Professor Dr. Yusuke Takezawa (The university of Tokyo) to give me useful suggestion about research.

I gratefully acknowledge all the members of Shionoya laboratory to support everyday of my research. Especially active discussion with Dr. Ryo Yamada, Dr. Hirotaka Yonezawa, Mr. Kenichi Endo, and Mr. Fumiya Iizuka are very helpful and inspiring. I would also like to thank Mr. Yutaro Yamashita for his kindly help concerning X-ray analysis. I would also like to thank Ms Tong Xing and Ms Yingjie Lin, for the support, care and laugh they bring to my life.

Finally I would like to express my gratitude to my beloved parents and boyfriend, who have always helping me out of difficulties and supporting without a word of complaint.